

hep-th/9612030
December 1996

DECONFINEMENT TRANSITION FOR QUARKS ON A LINE

C.R. Gattringer, L.D. Paniak and G.W. Semenoff

*Department of Physics and Astronomy,
University of British Columbia
6224 Agricultural Road
Vancouver, British Columbia, Canada V6T 1Z1*

Abstract

We examine the statistical mechanics of a 1-dimensional gas of both adjoint and fundamental representation quarks which interact with each other through 1+1-dimensional $U(N)$ gauge fields. Using large- N expansion we show that, when the density of fundamental quarks is small, there is a first order phase transition at a critical temperature and adjoint quark density which can be interpreted as deconfinement. When the fundamental quark density is comparable to the adjoint quark density, the phase transition becomes a third order one. We formulate a way to distinguish the phases by considering the expectation values of high winding number Polyakov loop operators.

1 Introduction

The classical Coulomb gas is an important model in statistical mechanics. It is exactly solvable in one dimension. In two dimensions it exhibits the Berezinsky-Kosterlitz-Thouless phase transition which is the prototype of all phase transitions in two-dimensional systems which have $U(1)$ symmetry. In this paper, we shall discuss a generalization of the classical Coulomb gas to a system of quarks which interact with each other through non-Abelian electric fields. This model is known to be exactly solvable in some special cases, for $SU(2)$ gauge group and fundamental representation quarks in one dimension [1] and for $SU(N)$ gauge group in the large- N limit with adjoint representation quarks in one dimension [2, 3]. It can also be formulated on the lattice and solved with adjoint quarks in the large N limit in higher dimensions [3, 4] where it has a substantially more complicated structure, although, even there, a solution of some special cases of the model are relevant to the deconfinement transition of three and four-dimensional Yang-Mills theory [5].

In the present paper, we shall concentrate on solving a more general version of the one-dimensional model than has previously been considered and elaborating on the properties of the solution. The one-dimensional case has the advantage of being directly related to a continuum field theory, the heavy quark limit of 1+1-dimensional quantum chromodynamics (QCD). Part of the motivation for this work is to study the possibility of a confinement-deconfinement phase transition at high temperature or density in a field theory which has some of the features of QCD, i.e. with similar gauge symmetries and where interactions are mediated by non-Abelian gauge fields. QCD exhibits confinement at low temperature and density with elementary excitations being color neutral particles - mesons and baryons. On the other hand, at high temperature or high density it is very plausible that the dynamical degrees of freedom would be quarks and gluons - which would form a quark-gluon plasma, rather than the mesons and baryons of low temperature nuclear physics. At some intermediate temperature or density there should be a crossover between these two regimes. There are few explicitly solvable models where this behavior can be studied directly. Previous to the model of [2, 3], known explicit examples of phase transitions in Yang-Mills theory were not associated with confinement, but were either lattice artifacts [6] unrelated to the continuum gauge theory or were associated with topological degrees of freedom in Yang-Mills theory on the sphere [7] and cylinder [5, 8] and demarcate a finite range of coupling constants within which the gauge theory resembles a string theory.

In finite temperature Yang-Mills theory (or QCD with only adjoint quarks), confinement is thought to be governed by the realization of a global symmetry which is related to the center of the gauge group and implemented by certain topologically non-trivial gauge transformations that appear only at finite temperature [9, 10, 11]. The Polyakov loop operator is an order parameter for spontaneous breaking of this center symmetry and yields a mathematical way of distinguishing the confining and deconfined phases. When fundamental representation quarks are present, the center symmetry is broken explicitly and the Polyakov loop operator

is no longer a good order parameter for confinement. Whether, in this case, a mathematical distinction of confined and deconfined phases exists, and indeed whether there is a distinct phase transition at all, is an open question.

Here, we will consider a toy model which resembles two-dimensional QCD with heavy adjoint and fundamental representation quarks. It could also be thought of as the heavy quark limit of dimensionally reduced higher dimensional QCD where the adjoint particles are the gluons of the compactified dimension which get a mass (similar to a Debye mass) from the dimensional reduction, and the fundamental representation particles are the quarks. We will solve this model explicitly in the large- N limit. The model with only adjoint quarks was solved in refs. [2, 3] and it was found that the explicit solution has a first order phase transition between confining and deconfining phases. These phases could be distinguished by the expectation value of the Polyakov loop operator, which provided an order parameter for confinement in that case. In this paper, we shall add fundamental representation quarks. Then, as in QCD, the center symmetry is explicitly broken and the Polyakov loop is always non-vanishing. We nevertheless find that the first order phase transition persists when the density of fundamental quarks is sufficiently small. When the density of fundamental quarks is increased until it is comparable to the density of adjoint quarks, the phase transition becomes a second order one. When the fundamental quark density is increased further, the phase transition is third order.

It is tempting to identify this third order phase transition as the vestige of the deconfinement transition. Indeed, we shall present arguments for this. We shall find a mathematical way to distinguish the phases on either side of the third order transition based on the behavior of Polyakov loops with high winding numbers. We conjecture that the generalization of this argument to higher dimensional systems would provide a mathematical characterization of confinement in finite temperature QCD with fundamental representation quarks.

Another motivation of the present paper, as well as Ref. [2, 3] is to study a suggestion by Kutasov [12] that 1+1-dimensional adjoint QCD would be the simplest gauge theory model which exhibits some of the stringy features of a confining gauge theory. It is a long-standing conjecture that the confining phase of a gauge theory can be described by a string theory [13]. There are only two cases where this relationship is well understood, two-dimensional Yang-Mills theory [14, 15, 16] and compact quantum electrodynamics [17]. At low temperatures 1+1-dimensional adjoint QCD is confining in the conventional sense that quarks only appear in the spectrum in color neutral bound states. This is a result of the fact that, in one dimension, the gluon field has no propagating degrees of freedom and therefore it cannot form a color singlet bound state with an adjoint quark. As a result, the quantum states are color singlet bound states of two or more adjoint quarks. The spectrum contains an infinite number of families of multi-quark bound states which resemble asymptotically linear Regge trajectories [12, 18, 19] and, for large energies, the density of states increases exponentially with energy [20]. This implies a Hagedorn transition [21] at high temperature. Kutasov [12]

supported this view by using an argument originally due to Polchinski [22] that a deconfinement transition occurs when certain winding modes become tachyonic at high temperature. This behaviour was a feature of the explicit first order deconfinement transition found in the model considered in [2, 3]. That model, which coincides with the heavy quark limit of adjoint QCD, is effectively a statistical mechanical model for strings of electric flux, with quarks attached to their ends.

The large- N expansion of two-dimensional adjoint QCD has the same complexity as the large- N expansion of a higher dimensional Yang-Mills theory and the leading order, infinite- N limit cannot be found analytically [23]. In fact, the dimensional reduction of three or four-dimensional Yang Mills theory produces two-dimensional QCD with massless adjoint scalar quarks, so the combinatorics of planar diagrams is very similar.

1.1 Overview

This paper is organized as follows: In Section 2.1 we identify the gauged principal chiral model which corresponds to the gas with sources in various representations. In Section 2.2 the quantum mechanical formulation of this unitary matrix model is analyzed. This is followed by a section (2.3) where we rewrite the model in terms of collective variables (eigenvalue density), which are convenient for analyzing the large- N limit.

Parametrized solutions to the collective field equations are given in Section 3.1, and the parametrized free energy and its derivatives are obtained in 3.2. We also show that they give rise to a first order differential equation the free energy has to obey. In Section 3.3 we establish the existence of a third order line in the phase diagram, and compute the point where it terminates. Using numerical techniques we show in 3.4 that the critical line continues from that point as a first order line.

In Section 4.1 we derive the contributions of the gauge field and the sources respectively to the energy density. This is followed by a section where we establish that higher windings of Polyakov loop operators behave differently in the two phases (4.2). This allows to discuss the phase diagram using energy densities and higher winding loop operators (4.3). The paper ends with a summary and outlook (4.4). Some of the more technical calculations are given in an appendix.

2 Formalism

2.1 Effective action

The partition function of 1+1-dimensional Yang-Mills theory at temperature T and coupled to a number K of non-dynamical quarks at positions x_1, \dots, x_K in representations R_1, \dots, R_K

of the gauge group is obtained by taking the thermal average of an ensemble of Polyakov loop operators

$$Z[T; x_1, \dots, x_K; R_1, \dots, R_K] = \int dA_\mu e^{-S[A]} \prod_{i=1}^K \text{Tr} \mathcal{P} e^{i \int_0^{1/T} d\tau A_0^{R_i}(\tau, x_i)} , \quad (2.1)$$

where the Euclidean action is

$$S[A] = \int_0^{1/T} d\tau \int dx \frac{1}{2e^2} \text{Tr} (F_{\mu\nu}(\tau, x))^2 , \quad (2.2)$$

the gauge fields are Hermitean $N \times N$ matrix valued vector fields which have periodic boundary conditions in imaginary time

$$A_\mu(\tau, x) = A_\mu(\tau + 1/T, x) ,$$

and the field strength is

$$F_{\mu\nu} \equiv \partial_\mu A_\nu - \partial_\nu A_\mu - i [A_\mu, A_\nu] .$$

The gauge field can be expanded in basis elements of the Lie algebra $A_\mu^{R_i} \equiv A_\mu^a T_{R_i}^a$ with $T_{R_i}^a$ the generators in the representation R_i . For concreteness, we consider $U(N)$ gauge theory and denote the generators in the fundamental representation as T^a with $a = 1, \dots, N^2$. They obey

$$[T^a, T^b] = i f^{abc} T^c , \quad (2.3)$$

normalized so that

$$\text{Tr} T^a T^b = \frac{1}{2} \delta^{ab} , \quad (2.4)$$

and with the sum rule

$$\sum_{a=1}^{N^2} T_{ij}^a T_{kl}^a = \frac{1}{2} \delta_{jk} \delta_{il} . \quad (2.5)$$

We remark that group elements g^{Ad} in the adjoint representation are related to the fundamental representation matrices g by

$$(g^{Ad})^{ab} = 2 \text{Tr}(g^\dagger T^a g T^b) . \quad (2.6)$$

The expression (2.1) can be obtained by canonical quantization of 1+1-dimensional Yang-Mills theory with Minkowski space action coupled to some non-dynamical sources

$$S = - \int dt dx \frac{1}{2e^2} \text{Tr} F_{\mu\nu} F^{\mu\nu} + \text{source terms} . \quad (2.7)$$

In the following, we will review an argument for representing the partition function of Yang-Mills theory as a gauged principal chiral model which was first given in [27] and which was generalized to the case of Yang-Mills theory with sources in [2, 3]. As is usual in canonical

quantization of a gauge theory, the canonical conjugate $E(x)$ of the spatial component of the gauge field (which we denote by $A(x)$), is proportional to the electric field,

$$E = \frac{1}{e^2} F_{01} ,$$

and obeys the commutation relation

$$[A^a(x), E^b(y)] = i\delta^{ab}\delta(x - y) . \quad (2.8)$$

The Hamiltonian is

$$H = \int dx \frac{e^2}{2} \sum_{a=1}^{N^2} (E^a(x))^2 . \quad (2.9)$$

This Hamiltonian must be supplemented by the Gauss' law constraint equation which is the equation of motion for A_0 following from (2.7) and which contains the color charge densities of the sources

$$\mathcal{G}^a(x) \equiv \left(\frac{d}{dx} E^a(x) - f^{abc} A^b(x) E^c(x) + \sum_{i=1}^K T_{R_i}^a \delta(x - x_i) \right) \sim 0 . \quad (2.10)$$

Here, the particles with color charges are located at positions x_1, \dots, x_K . $T_{R_i}^a$ are generators in the representation R_i operating on the color degrees of freedom of the i 'th particle.

There are two options for imposing this constraint. The first is to impose another gauge fixing condition such as

$$A \sim 0 ,$$

and to use the constraints to eliminate both E and A . The resulting Hamiltonian is

$$H = \sum_{i < j, a} \frac{e^2 N}{4} T_{R_i}^a \otimes T_{R_j}^a |x_i - x_j| , \quad (2.11)$$

which was considered in Ref. [1]. It is the energy of an infinite range spin model where the spins take values in the Lie algebra of $U(N)$.

The other option, which makes the closest contact with string dynamics, is to impose the constraint (2.10) as a physical state condition,

$$\mathcal{G}^a(x) \Psi_{\text{phys}} = 0 .$$

To do this, it is most illuminating to work in the functional Schrödinger picture, where the states are functionals of the gauge field, $\psi[A]$ and the electric field is the functional derivative operator

$$E^a(x) \Psi[A] = \frac{1}{i} \frac{\delta}{\delta A^a(x)} \Psi[A] ,$$

The time-independent functional Schrödinger equation is

$$\int dx \left(-\frac{e^2}{2} \sum_{a=1}^{N^2} \frac{\delta^2}{(\delta A^a(x))^2} \right) \Psi^{a_1 \dots a_K} [A; x_1, \dots, x_K] = \mathcal{E} \Psi^{a_1 \dots a_K} [A; x_1, \dots, x_K] .$$

Gauss' law implies that the physical states, i.e. those which obey the gauge constraint (2.10), transform as

$$\Psi^{a_1 \dots a_K} [A^g; x_1, \dots, x_K] = g_{a_1 b_1}^{\text{R}_1}(x_1) \dots g_{a_K b_K}^{\text{R}_K}(x_K) \Psi^{b_1 \dots b_K} [A; x_1, \dots, x_K] ,$$

where

$$A^g \equiv g A g^\dagger - i g \nabla g^\dagger ,$$

is the gauge transform of A .

For a fixed number of particles, the quantum mechanical problem is exactly solvable. For example, the wavefunction of a fundamental representation quark-antiquark pair is

$$\Psi^{ij} [A; x_1, x_2] = \left(\mathcal{P} e^{i \int_{x_1}^{x_2} dy A(y)} \right)^{ij} , \quad (2.12)$$

where the path ordered phase operator represents a string of electric flux connecting the positions of the quark and anti-quark. The energy is $\frac{e^2 N}{4} |x_1 - x_2|$. For a pair of adjoint quarks, the wavefunction is

$$\Psi^{ab} [A; x_1, x_2] = \text{Tr} \left(T^a \mathcal{P} e^{i \int_{x_1}^{x_2} A} T^b \mathcal{P} e^{i \int_{x_2}^{x_1} A} \right) . \quad (2.13)$$

with energy $\frac{e^2 N}{2} |x_2 - x_1|$. These energy states are identical to what would be obtained by diagonalizing the 'spin' operators in the gauge fixed Hamiltonian (2.11).

Note that the wavefunctions (2.12) and (2.13) are not normalizable by functional integration over A . This is a result of the fact that the gauge freedom has not been entirely fixed, so that the normalization integral still contains the infinite factor of the volume of the group of static gauge transformations.

In general, for a fixed distribution of quarks, a state-vector is constructed by connecting them with appropriate numbers of strings of electric flux so that the state is gauge invariant. The number of ways of doing this fixes the dimension of the quantum Hilbert space. If the flux strings overlap, the Hamiltonian can mix different configurations, so the energy eigenstates are superpositions of string configurations. However, this mixing is suppressed in the large- N limit (i.e. the strings are non-interacting) and any string distribution is an eigenstate of the Hamiltonian with eigenvalue $(e^2 N/4) \times (\text{total length of all strings})$.

We shall study the thermodynamics of this system by constructing the partition function. We work with the grand canonical ensemble and assume that the quarks obey Maxwell-Boltzmann statistics. The partition function of a fixed number of quarks is constructed by taking the trace of the Gibbs density $e^{-H/T}$ over physical states. This can be implemented by considering set of all states in the representation of the commutator (2.8), spanned by, for example, the eigenstates of $A^a(x)$ and an appropriate basis for the quarks

$$|A\rangle \otimes e_{a_1} \otimes e_{a_2} \otimes \dots \otimes e_{a_K} .$$

Projection onto physical, gauge invariant states is done by gauge transforming the state at one side of the trace and then integrating over all gauge transformations (and then dividing by the infinite volume of the gauge group) [26]. The resulting partition function is

$$Z[T/e^2; x_1, \dots, x_K] = \int [dA][dg] \langle A | e^{-H/T} | A^g \rangle \text{Tr } g^{R_1}(x_1) \dots \text{Tr } g^{R_K}(x_K) , \quad (2.14)$$

where $[dg]$ is the Haar measure on the space of mappings from the line to the group manifold and $[dA]$ is a measure on the convex Euclidean space of gauge field configurations. The expression (2.14) is identical to (2.1) with the Polyakov loop operator is the trace of the group element $g(x)$ in the appropriate representation.

In going over to the grand canonical ensemble the first step is to integrate over all particle positions. We then multiply by the fugacities for each type of charge: a factor of λ_R for each quark in representation R . To impose Maxwell-Boltzmann statistics, we divide by the factorial of the number of quarks in each representation. We then sum over all numbers of quarks in each representation. This exponentiates the fugacities, resulting in the grand partition function

$$Z[T/e^2, \lambda_R] = \int [dA][dg] e^{-S_{\text{eff}}[A, g]} , \quad (2.15)$$

where the effective action is

$$\exp(-S_{\text{eff}}[A, g]) = \langle A | e^{-H/T} | A^g \rangle \exp\left(\int dx \sum_R \lambda_R \text{Tr } g^R(x)\right) , \quad (2.16)$$

and the summation in the exponent is over all the irreducible representations of $U(N)$ we want to consider. The Hamiltonian is the Laplacian on the space of gauge fields. The heat kernel obeys the equation

$$\left(T^2 \frac{\partial}{\partial T} + \int dx \frac{e^2}{2} \sum_{a=1}^{N^2} \left(\frac{\delta}{\delta A^a(x)}\right)^2\right) \langle A | e^{-H/T} | A^g \rangle = 0 ,$$

with the boundary condition

$$\lim_{1/T \rightarrow 0} \langle A | e^{-H/T} | A^g \rangle = \delta(A - A^g) .$$

These equations are easily solved by a Gaussian - divided by a T -dependent constant:

$$\langle A | e^{-H/T} | A^g \rangle \sim \exp\left(-\int dx \frac{T}{e^2} \text{Tr } (A - A^g)^2\right) .$$

We see that the effective theory is the gauged principal chiral model with a potential energy term for the group-valued degrees of freedom,

$$S_{\text{eff}}[A, g] = \int dx \left(\frac{N}{2\gamma} \text{Tr} |\nabla g(x) + i[A(x), g(x)]|^2 - \sum_R (\lambda_R \text{Tr } g^R(x)) \right) . \quad (2.17)$$

Note that we have introduced the coupling constant

$$\gamma \equiv \frac{e^2 N}{2T}. \quad (2.18)$$

When we analyze the limit $N \rightarrow \infty$, we will tune e^2 such that γ is constant. Moreover, we assume that the fugacities λ_R are scaled such that all terms in the action (2.17) are of order N^2 .

The potential energy term in the effective action,

$$V(g) \equiv - \sum_R \lambda_R \text{Tr} \left(g^R(x) \right), \quad (2.19)$$

is the expansion of a local class function of the group element $g(x)$ (one which obeys $V(g) = V(hgh^{-1})$ for $h \in U(N)$) in group characters with coefficients λ_R . The characters

$$\chi_R(g) \equiv \text{Tr} \left(g^R(x) \right),$$

form a complete set of orthonormal class functions of the group variable, with inner product

$$\int [dg] \chi_R^*(g) \chi_{R'}(g) = \delta_{R,R'}.$$

Here $[dg]$ is not a functional integral measure, but is the Haar measure for integration on $U(N)$. From the potential, we can find a fugacity by

$$\lambda_R = - \int [dg] \chi_R^*(g) V(g).$$

By tuning the fugacities appropriately, we could obtain any local invariant potential.

The effective action (2.17) with all $\lambda_R = 0$ was discussed by Grignani et.al. [27] and was solved explicitly in the limit $N \rightarrow \infty$ by Zarembo [4]. The model with $\lambda_{Ad} \neq 0$ (with adjoint quarks) was solved in Refs.[2] and [3]. The effective action (2.17) is gauge invariant,

$$S_{\text{eff}}[A, g] = S_{\text{eff}}[A^h, hgh^\dagger].$$

It is also covariant under the global transformation

$$S_{\text{eff}}[A, zg, \lambda_R] = S_{\text{eff}}[A, g, z^{-C_1(R)} \lambda_R]. \quad (2.20)$$

where z is a constant element from the center of the gauge group, which for $U(N)$ is $\sim U(1)$ and would be the discrete group Z_N for gauge group $SU(N)$. Here, $C_1(R)$ is the linear Casimir invariant of the representation R , which is the number of boxes in the Young tableau corresponding to R . When the gauge group is $SU(N)$ and the only non-zero fugacities are for the zero ‘N-ality’ representations, i.e. those for which $C_1(R) = 0 \bmod N$, there is a global Z_N symmetry. For gauge group $U(N)$, this occurs only when all representations with non-zero fugacities have equal numbers of quarks and anti-quarks. The fugacities of other non-symmetric charges, can be thought of as an external field which breaks the center symmetry of the system explicitly. This situation is akin to the effect of an external magnetic field on a spin system.

2.2 Matrix quantum mechanics

If we re-interpret x as Euclidean time, the partition function that we have derived has the form of a Euclidean space representation of the partition function for matrix quantum mechanics, where the free energy is identical to the ground state energy of the matrix quantum mechanics. We can study the latter model by mapping the problem to real time τ by setting $x = i\tau$ and $A \rightarrow -iA$. The action in real time is then

$$S_{QM} = \int d\tau \left(\frac{N}{2\gamma} \text{Tr} |\dot{g} + i[A, g]|^2 - V(g) \right).$$

We remark that this action must not be confused with the action (2.2). S_{QM} is the action for a 0+1-dimensional problem (quantum mechanics), while (2.2) is the action for Yang Mills theory in 1+1 dimensions. This remark also holds for the Hamiltonian below. In order to avoid confusion, we label the quantum mechanical quantities with the subscript QM .

The canonical momentum conjugate to the group valued position variable g is the Lie algebra element

$$\Pi = \frac{N}{\gamma} (ig^\dagger \dot{g} + g^\dagger A g - A),$$

and the Hamiltonian is

$$H_{QM} = \frac{\gamma}{2N} \text{Tr} \Pi^2 - \frac{\gamma}{N} \text{Tr} \Pi (g^\dagger A g - A) + V(g). \quad (2.21)$$

The gauge field A plays the role of a Lagrange multiplier which enforces the constraint

$$g \Pi g^\dagger - \Pi \sim 0,$$

and the Hamiltonian reduces to

$$H_{QM} = \frac{\gamma}{2N} \text{Tr} \Pi^2 + V(g).$$

We can expand the canonical momentum as

$$\Pi = \sum_a \Pi^a T^a,$$

Then, the components satisfy the Lie algebra

$$[\Pi^a, \Pi^b] = i f^{abc} \Pi^c, \quad (2.22)$$

$$[\Pi^a, g] = g T^a, \quad (2.23)$$

$$[\Pi^a, g^\dagger] = -T^a g^\dagger. \quad (2.24)$$

It follows that in the Schrödinger picture the components of the canonical momentum are represented as

$$\Pi^a = \text{Tr} g T^a \frac{\partial}{\partial g} = g_{ij} T^a_{jk} \frac{\partial}{\partial g_{ik}}.$$

Denoted in components the constraint reads

$$G^a \equiv \left(\text{Tr} T^a g T^b g^\dagger - \frac{1}{2} \delta^{ab} \right) \Pi^b \sim 0 .$$

The constraint has no operator ordering ambiguity. It generates the adjoint action of the symmetry group

$$[G^a, g] = \frac{1}{2} [T^a, g] .$$

The constraint can be realized as a physical state condition

$$G^a \psi_{\text{phys}} = 0 .$$

In the representation where states are functions of g , this implies that the physical states are class functions

$$\psi_{\text{phys}}(g) = \psi_{\text{phys}}(hgh^{-1}) ,$$

where $h \in U(N)$. This means that the physical states are functions of the eigenvalues of g .

In a basis where g is diagonal,

$$g = \begin{pmatrix} e^{i\alpha_1} & 0 & 0 & 0 & \dots & 0 \\ 0 & e^{i\alpha_2} & 0 & 0 & \dots & 0 \\ 0 & 0 & e^{i\alpha_3} & 0 & \dots & 0 \\ 0 & 0 & \dots & & & 0 \\ 0 & 0 & \dots & & & e^{i\alpha_N} \end{pmatrix} , \quad (2.25)$$

the wavefunctions are functions of α_i ,

$$\psi_{\text{phys}}(\alpha_1, \dots, \alpha_N) = \psi_{\text{phys}}(\alpha_1, \dots, \alpha_i + 2\pi, \alpha_N) . \quad (2.26)$$

Denoting the gauge group Laplacian in components

$$\Delta \equiv \sum_{a=1}^{N^2} (\Pi^a)^2 , \quad (2.27)$$

the Hamiltonian reads

$$H_{QM} = \frac{\gamma}{4N} \Delta + V(g) .$$

Since the potential $V(g)$ is also a class function and depends only on the eigenvalues, when operating on the physical states, the Hamiltonian can be expressed in terms of eigenvalues and derivatives by eigenvalues

$$H_{QM} = \frac{\gamma}{4N} \frac{1}{\tilde{J}(\alpha)} \left(\sum_1^N -\frac{\partial^2}{\partial \alpha_i^2} - N(N^2 - 1)/12 \right) \tilde{J}(\alpha) + V(\alpha) ,$$

where

$$\tilde{J}(\alpha) = \prod_{i < j} 2 \sin \frac{1}{2} (\alpha_i - \alpha_j) = \frac{1}{(2i)^{N(N-1)/2}} \frac{J(\alpha)}{\prod_i z_i^{(N-1)/2}} ,$$

and

$$J(z) = \prod_{i < j} (z_i - z_j) \quad , \quad z_i \equiv e^{i\alpha_i} .$$

The physical states must be symmetric functions of α_i . (There is a residual gauge invariance [28] under the Weyl group which permutes the eigenvalues and the physical state condition requires that the physical states be symmetric under these permutations.) The normalization integral for the wavefunction is

$$\int [dg] \psi^\dagger(g) \psi(g) = 1 .$$

Since the integrand depends only on the eigenvalues of g , It is convenient to write the Haar measure as an integral over eigenvalues of g with the Jacobian which is the Vandermonde determinant,

$$\int \left(\prod_i d\alpha_i \right) |\tilde{J}(\alpha)|^2 \psi^\dagger(\alpha) \psi(\alpha) = 1 .$$

The Hamiltonian and inner product have a particularly simple form when we redefine the wavefunction as

$$\tilde{\psi}(\alpha_1, \dots, \alpha_N) \equiv \tilde{J}(\alpha) \psi(\alpha_1, \dots, \alpha_N) .$$

Since \tilde{J} is antisymmetric, $\tilde{\psi}$ is a completely antisymmetric function of the eigenvalues, which we can think of as the coordinates of fermions. The Hamiltonian is that of an interacting Fermi gas

$$\left\{ \frac{\gamma}{4N} \left(\sum_1^N -\frac{\partial^2}{\partial \alpha_i^2} - N(N^2 - 1)/12 \right) + V(\alpha) \right\} \tilde{\psi}(\alpha) = \mathcal{E} \tilde{\psi}(\alpha) .$$

This correspondence of a c=1 matrix model with a Fermi gas was first pointed out in Ref. [29].

2.3 Large N: Collective variables

In this section we shall examine the collective field formulation of the large- N limit of the theory that we discussed in the last subsection [4, 30]. The Hamiltonian obtained in the last subsection reads

$$H_{QM} = \frac{\gamma}{4N} \sum_{a=1}^{N^2} (\Pi^a)^2 + V(g) , \quad (2.28)$$

with (compare (2.19))

$$V(g) \equiv - \sum_R \lambda_R \text{Tr} \left(g^R(\tau) \right) .$$

It was shown (compare (2.25),(2.26)) that the wavefunction depends only on the eigenvalues $e^{i\alpha_j}$ of g and thus the density of eigenvalues

$$\rho(\theta, \tau) \equiv \frac{1}{N} \sum_{i=1}^N \delta(\theta - \alpha_i(\tau)) ,$$

completely characterizes the properties of the system. Interpretation of the physics of the system at large N is more convenient when one considers the Fourier transform of the eigenvalue distribution

$$\rho(\theta, \tau) = \frac{1}{2\pi} + \frac{1}{2\pi} \sum_{n \neq 0} c_n(\tau) e^{-in\theta}, \quad (2.29)$$

where we have defined

$$c_n(\tau) \equiv \frac{1}{N} \text{Tr} g^n(\tau) \quad , \quad c_{-n}(\tau) = \overline{c_n(\tau)}.$$

We now turn our attention to developing the collective field theory formulation of the (thermo-) dynamical problem given by the Hamiltonian (2.28). Since the wavefunction depends only on the eigenvalues of g , we would like a Hamiltonian equivalent to (2.28) but written in terms of the eigenvalue density ρ and a conjugate momentum Π . At large N we will find this Hamiltonian and write equations of motion for ρ and Π . So far we have not imposed any restriction on the potential $V(g)$, but from now on we assume, that it can be expressed as a functional of the eigenvalue density $\rho(\theta)$. In particular the potential we are going to analyze below will have this property.

The canonical momentum operates on the wavefunction as

$$\begin{aligned} \Pi^a \psi[\rho] &= \int d\theta [\Pi^a, \rho(\theta)] \frac{\delta}{\delta \rho(\theta)} \psi[\rho] \\ &= \frac{1}{2\pi N} \int d\theta \sum_K e^{-iK\theta} K \text{Tr}(T^a g^K) \frac{\delta}{\delta \rho(\theta)} \psi[\rho], \end{aligned}$$

and the Laplacian (2.27) is

$$\begin{aligned} \Delta \psi[\rho] &= \left(\frac{1}{4\pi N} \int d\theta \sum_K e^{-iK\theta} |K| \left(\sum_{L=0}^K \text{Tr} g^L \text{Tr} g^{K-L} - N \text{Tr} g^K \right) \frac{\delta}{\delta \rho(\theta)} \right. \\ &\quad \left. + \frac{1}{8\pi^2 N^2} \int d\theta d\theta' \sum_{KL} K L e^{-iK\theta - iL\theta'} \text{Tr} g^{K+L} \frac{\delta^2}{\delta \rho(\theta) \delta \rho(\theta')} \right) \psi[\rho], \end{aligned}$$

which can be written as

$$\begin{aligned} \Delta \psi[\rho] &= -\frac{1}{2N} \int d\theta \rho(\theta) \left\{ \left(\frac{\partial}{\partial \theta} \frac{\delta}{\delta \rho(\theta)} \right)^2 - N^2 \mathcal{P} \int d\theta' \rho(\theta') \cot\left(\frac{\theta - \theta'}{2}\right) \frac{\partial}{\partial \theta} \frac{\delta}{\delta \rho(\theta)} \right\} \psi[\rho] \\ &= -\frac{1}{2N} \int d\theta \rho(\theta) \left(\left(\frac{\partial}{\partial \theta} \frac{\delta}{\delta \rho(\theta)} + \mathcal{V}(\theta) \right)^2 - \mathcal{V}^2(\theta) \right) \psi[\rho], \end{aligned}$$

where

$$\mathcal{V}(\theta) = \frac{N^2}{2} \mathcal{P} \int d\theta' \rho(\theta') \cot\left(\frac{\theta - \theta'}{2}\right).$$

\mathcal{P} indicates principal value integral.

The transformation of the wavefunction

$$\psi[\rho] = \tilde{\psi}[\rho] \exp \left(-\frac{N^2}{2} \int d\theta d\theta' \ln \sin \frac{|\theta - \theta'|}{2} \rho(\theta) \rho(\theta') \right) ,$$

transforms the derivative in the Schrödinger equation so that it has the form

$$\left\{ -\frac{\gamma}{8N^2} \int d\theta \rho(\theta) \left\{ \left(\frac{\partial}{\partial \theta} \frac{\delta}{\delta \rho(\theta)} \right)^2 - \mathcal{V}^2(\theta) \right\} + V[\rho] \right\} \tilde{\psi}[\rho] = E \tilde{\psi}[\rho] . \quad (2.30)$$

The second term on the left-hand-side of this equation has a simple form. In Appendix A.1 it is shown that it gives rise to a term which is cubic in the density. Thus, the Schrödinger equation has the form

$$\left\{ -\frac{\gamma}{8N^2} \int d\theta \left(\rho(\theta) \left(\frac{\partial}{\partial \theta} \frac{\delta}{\delta \rho(\theta)} \right)^2 - N^4 \frac{\pi^2}{3} \rho^3(\theta) \right) + V[\rho] \right\} \tilde{\psi}[\rho] = E \tilde{\psi}[\rho] , \quad (2.31)$$

up to an overall constant.

The large- N limit is dominated by the eikonal approximation. In this approximation, we make the ansatz for the wavefunction

$$\tilde{\psi}[\rho] = \exp(iN^2 S[\rho]) .$$

The eikonal, S then obeys the equation

$$\frac{H_{QM}[\rho, \Pi]}{N^2} = \frac{\gamma}{8} \int d\theta \left\{ \rho(\theta) \left(\frac{\partial}{\partial \theta} \frac{\delta S}{\delta \rho(\theta)} \right)^2 + \frac{\pi^2}{3} \rho^3(\theta) \right\} + \frac{1}{N^2} V[\rho] = \frac{E}{N^2} . \quad (2.32)$$

Here, we have ignored a term which is of subleading order in N^2 . We have also assumed that $V[\rho]$ will be of order N^2 (compare Section 2.1) and that the natural magnitude of the energy eigenvalue is of order N^2 .

To solve this equation for the ground state, we must find its minimum by varying ρ and the canonical momentum

$$\Pi = \delta S / \delta \rho ,$$

subject to the condition that ρ is normalized. This leads to the equations of collective field theory

$$\begin{aligned} \frac{\partial}{\partial \tau} \rho(\tau, \theta) &= \frac{\delta H_{QM}/N^2}{\delta \Pi(\tau, \theta)} , \\ \frac{\partial}{\partial \tau} v(\tau, \theta) &= -\frac{\partial}{\partial \theta} \frac{\delta H_{QM}/N^2}{\delta \rho(\tau, \theta)} , \end{aligned}$$

where

$$v(\tau, \theta) \equiv \frac{\partial}{\partial \theta} \Pi(\tau, \theta) .$$

Taking the derivative of the second equation with respect to θ eliminates a Lagrange multiplier which must be introduced in order to enforce the normalization condition for ρ . Using (2.32) one finds

$$\begin{aligned} \frac{\partial}{\partial \tau} \rho + \frac{\gamma}{4} \frac{\partial}{\partial \theta} (\rho v) &= 0, \\ \frac{\partial}{\partial \tau} v + \frac{\gamma}{8} \frac{\partial}{\partial \theta} (v^2 + \pi^2 \rho^2) + \frac{1}{N^2} \frac{\partial}{\partial \theta} \frac{\delta}{\delta \rho} V[\rho] &= 0. \end{aligned} \quad (2.33)$$

It is interesting to note that these are nothing but Euler's equations for a fluid with equation of state $P = \pi^2 \rho^3/3$ on a cylinder with coordinates (θ, τ) . The inclusion of a potential $V(\theta, \tau)$ corresponding to non-Abelian charges is equivalent to subjecting the fluid to an external force which is derived from $V(\theta, \tau)$.

We shall use these equations in the next section where we analyze the large- N limit of a mixed gas of adjoint and fundamental charges.

3 Free energy and critical behaviour

3.1 Static solutions to the collective field equations

In this section we will find static solutions to the collective field equations (2.33). The most simple potentials involve only the lowest representations, the fundamental, its conjugate and the adjoint. We shall consider a slight generalization of these and use powers of the lowest representations to include multiple windings of the Polyakov loop operator. Our potential reads¹

$$V(g) \equiv - \sum_{n=1}^{\infty} \left(\kappa_n N \text{Tr}(g^n) + \bar{\kappa}_n N \text{Tr}((g^\dagger)^n) + \lambda_n |\text{Tr} g^n|^2 \right), \quad (3.1)$$

where we made use of (compare (2.5), (2.6))

$$\text{Tr} (g^{Ad}(x))^n = |\text{Tr} g^n(x)|^2,$$

to relate the trace in the adjoint representation to the trace in the fundamental representation. The couplings for the fundamental representation charges (and their conjugates) were chosen to scale $\sim N$, to make the potential of order N^2 .

The potential (3.1) indeed can be expressed as a functional of the eigenvalue density (2.29). The collective field Hamiltonian (2.32) then reads

$$\begin{aligned} \frac{H_{QM}}{N^2} &= \frac{\gamma}{8} \int d\theta \left[\rho(\theta) (v(\theta))^2 + \frac{\pi^2}{3} \rho^3(\theta) \right] \\ &\quad - \sum_{n=1}^{\infty} \left(\lambda_n \left| \int d\theta \rho(\theta) e^{in\theta} \right|^2 + \kappa_n \int d\theta \rho(\theta) e^{in\theta} + \bar{\kappa}_n \int d\theta \rho(\theta) e^{-in\theta} \right) - \frac{\gamma}{96}. \end{aligned} \quad (3.2)$$

¹It should be remarked that parts of this section can easily be extended to more general potentials.

In order to maintain correspondence with the original version of the Hamiltonian (2.28) we subtract the constant $\gamma/96$. It sets the energy scale such that the free energy vanishes in the confined phase of the model with only adjoint charges (see below).

The corresponding collective field equations (2.33) read

$$\frac{\partial \rho}{\partial x} + \frac{\gamma}{4} \frac{\partial}{\partial \theta} (\rho v) = 0, \quad (3.3)$$

$$\frac{\partial v}{\partial x} + \frac{\gamma}{8} \frac{\partial v^2}{\partial \theta} - \frac{\pi^2 \gamma}{8} \frac{\partial \rho^2}{\partial \theta} + \frac{\partial}{\partial \theta} \sum_n \left[(\lambda_n c_{-n} + \kappa_n) e^{in\theta} + (\lambda_n c_n + \bar{\kappa}_n) e^{-in\theta} \right] = 0. \quad (3.4)$$

where c_n are the x -dependent Fourier coefficients of ρ as introduced in (2.29). Note that we also performed the change of variables, $\tau \rightarrow -ix$ and $v \rightarrow iv$ in these equations in order to invert the Wick rotation performed at the beginning of Section 2.2 prior to canonical quantization.

We will only consider real, static solutions of the non-linear equations (3.4), that is, where $\rho(\theta, x) = \rho_0(\theta)$ and the velocity v vanishes identically. Consequently

$$\rho_0(\theta) = \begin{cases} 2\sqrt{\frac{2}{\gamma\pi^2}}\sqrt{E + \sum(\lambda_n c_{-n} + \kappa_n)e^{in\theta} + \sum(\lambda_n c_n + \bar{\kappa}_n)e^{-in\theta}} & \text{where } \rho \text{ is real} \\ 0 & \text{otherwise} \end{cases}. \quad (3.5)$$

The constant of integration E has physical interpretation as the Fermi energy of a collection of N fermions [29] in the potential $V[\rho]$ and is fixed by the normalization condition

$$1 = \int d\theta \rho_0(\theta). \quad (3.6)$$

Here it is more convenient to express the c_n in terms of ρ_0 (compare (2.29))

$$c_n = \int d\theta \rho_0(\theta) e^{in\theta}. \quad (3.7)$$

The real support of the function $\rho_0(\theta)$ is the positive support of $\Lambda \equiv E + \sum(\lambda_n c_{-n} + \kappa_n)e^{in\theta} + \sum(\lambda_n c_n + \bar{\kappa}_n)e^{-in\theta}$. The zeros of Λ define the edges of the eigenvalue distribution and when these zeros condense one has critical behaviour in the observables of the model as in general Hermitean and unitary matrix models.

3.2 A differential equation for the free energy

In this subsection we compute all first order derivatives of the free energy and show that they obey a differential equation of the Clairaut type.

Inserting the static solution (3.5) in (3.2) we obtain for the free energy

$$\frac{1}{N^2} \langle H_{QM} \rangle \equiv f = \frac{1}{3} E - \frac{1}{3} \sum_{n=1}^{\infty} \left[\lambda_n |c_n|^2 + 2(\kappa_n c_n + \bar{\kappa}_n c_{-n}) \right] - \frac{\gamma}{96}. \quad (3.8)$$

Note that f is the leading coefficient ($O(N^2)$) of the energy for the matrix quantum mechanics problem, but for the quark gas problem plays the role of the leading coefficient of the energy *density*.

Deriving the expression (3.8) with respect to λ_J for some fixed J and using derivatives of Equations (3.6) and (3.7) with respect to the same parameter one obtains

$$\frac{df}{d\lambda_J} = -|c_J|^2. \quad (3.9)$$

We use the notation $d/d\lambda_J$ to indicate that also the c_n and E which implicitly depend on λ_J are derived with respect to this coupling. Similarly one can show

$$\frac{df}{d\kappa_J} = -c_J, \quad (3.10)$$

and

$$\frac{df}{d\gamma} = \frac{1}{3\gamma}E + \frac{1}{3\gamma} \sum_{n=1}^{\infty} [2\lambda_n|c_n|^2 + \kappa_n c_n + \bar{\kappa}_n c_{-n}] - \frac{1}{96}. \quad (3.11)$$

It is interesting to notice, that combining Equations (3.9) - (3.11) gives rise to a first order differential equation of the Clairaut type

$$\gamma \frac{df}{d\gamma} + \sum_{n=1}^{\infty} \left[\lambda_n \frac{df}{d\lambda_n} + \kappa_n \frac{df}{d\kappa_n} + \bar{\kappa}_n \frac{df}{d\bar{\kappa}_n} \right] = f. \quad (3.12)$$

This differential equation has general solutions of the form

$$f(\gamma, \lambda_n, \kappa_n) = \gamma F\left(\frac{\lambda_n}{\gamma}, \frac{\kappa_n}{\gamma}\right),$$

where F is some arbitrary smooth function. This result shows that the parameter γ is not driving the physical properties of the model, but rather sets the energy scale. The differential equation (3.12) gives no further restrictions on the function F and another analysis will be adopted in the next section. However, when finding the physical interpretation of the phase diagram in Section 4.3, the differential equation (3.8) will be a valuable tool.

3.3 Regime of the third order phase transition

We now restrict ourselves to the case of only one pair of non-vanishing couplings $\lambda_J, \kappa_J \neq 0$. Furthermore it is sufficient to consider κ_J real, since an eventual phase of κ_J can always be removed by using the covariance (2.20) of the action and Haar measure $[dg]$ under transformations by a constant element of $U(1)$.

In the form of (3.5) it is evident we need to solve simultaneously for the normalization condition (3.6) and the Fourier moment (3.7) in order to have a self-consistent solution of the saddle-point equations. We begin by introducing an auxiliary complex parameter

$$r_J e^{iJ\beta_J} \equiv \lambda_J c_{-J} + \kappa_J, \quad (3.13)$$

and rescaling the Fermi energy as

$$E \equiv 2\mu r_J. \quad (3.14)$$

With this notation the normalization and moment equations are respectively

$$1 = 2\sqrt{\frac{r_J}{\gamma}} I(\mu) \quad , \quad c_J e^{iJ\beta} = 2\sqrt{\frac{r_J}{\gamma}} M(\mu) , \quad (3.15)$$

where we have defined the integrals

$$\begin{aligned} I(\mu) &\equiv \frac{2}{\pi} \int_{-\pi}^{\pi} \sqrt{\mu + \cos(J\theta)} H(\mu + \cos(J\theta)) d\theta , \\ M(\mu) &\equiv \frac{2}{\pi} \int_{-\pi}^{\pi} \cos J\theta \sqrt{\mu + \cos(J\theta)} H(\mu + \cos(J\theta)) d\theta . \end{aligned} \quad (3.16)$$

Here $H(\cdot)$ denotes the step function. A simple transformation of the integration variable shows that $I(\mu)$ and $M(\mu)$ are independent of J . Thus J enters only as the subscript of the parameters. For notational convenience we abbreviate

$$\lambda_J \equiv \lambda \quad , \quad \kappa_J e^{-iJ\beta_J} \equiv \kappa . \quad (3.17)$$

We remark that $I(\mu)$, $M(\mu)$, and thus $c_J e^{iJ\beta_J}$ are real. Eliminating the moment c_J from (3.15) by using the definition (3.13) we obtain

$$\frac{\kappa}{\gamma} = \frac{1}{I(\mu)^2} \left[\frac{1}{4} - \frac{\lambda}{\gamma} I(\mu) M(\mu) \right] . \quad (3.18)$$

This family of lines in the κ, λ -plane parametrized by μ represent a necessary condition which a solution of the normalization and moment equations (3.15) must obey. From the last equation it is obvious that also the product $\kappa = \kappa_J e^{-iJ\beta}$ is real (thus $e^{iJ\beta}$ is just a sign). It occurs as a natural parameter when rewriting the free energy in terms of $I(\mu)$ and $M(\mu)$ (use (3.8))

$$f = \frac{\gamma}{12I(\mu)^2} \left[2\mu - \frac{M(\mu)}{I(\mu)} \right] - \kappa \frac{M(\mu)}{I(\mu)} - \frac{\gamma}{96} , \quad (3.19)$$

where we have eliminated λ using the necessary condition (3.18). Also the first derivative of the free energy with respect to κ can be expressed conveniently in terms of $I(\mu)$ and $M(\mu)$

$$\frac{df}{d\kappa} = -2 \frac{M(\mu)}{I(\mu)} . \quad (3.20)$$

Remember that we restricted ourselves to κ_J real, and thus we encounter a factor 2 compared to 3.10), since a real κ_J is the same for both terms c_J and c_{-J} in the potential (3.8).

With the parametric solution (3.8) at hand we turn our attention to establishing the critical behaviour in this model. In the appendix it is shown that the first derivatives of $I(\mu)$ and $M(\mu)$ have non-analytic behaviour at $\mu = 1$, hence the expression (3.20) suggests that the vicinity of $\mu = 1$ is a natural place to look for non-analytic behaviour in the free energy of

our model. Using the explicit results (A.5) for $I(1)$, $M(1)$ and (3.18) we obtain the necessary condition for the critical ($\mu = 1$) values of λ and κ

$$\frac{\kappa^c}{\gamma} = \frac{\pi^2}{512} - \frac{1}{3} \frac{\lambda^c}{\gamma}. \quad (3.21)$$

Having identified a line in the phase space where we expect critical behaviour we will now proceed to establish the details of this critical behaviour. Following [31] we begin by expanding about $\mu = 1$ and the line (3.21)

$$\mu = 1 + \varepsilon, \varepsilon > 0, \quad I(1 + \varepsilon) = I_c + \delta I, \quad M(1 + \varepsilon) = M_c + \delta M, \quad (3.22)$$

($I_c \equiv I(1)$, $M_c \equiv M(1)$) and analyze the variation of κ around κ^c while keeping λ fixed

$$\kappa = \kappa^c + \delta\kappa, \quad \lambda = \lambda^c. \quad (3.23)$$

Due to the nontrivial support of the integrands in (3.16) in principle one has to distinguish the cases $\mu > 1$ and $\mu < 1$; (see the appendix for details). In order to keep the formulas simple, we explicitly analyze only the case $\mu > 1$ as given by (3.22), (3.23). The case $\mu < 1$ can be treated along the same lines and we denote the corresponding results in the end.

The expansion now consists of two steps. We first expand the necessary condition (3.18) at $\mu = 1$ to obtain the relation between the variation $\delta\kappa$ and ε . In the second step we expand the right hand side of (3.20) at $\mu = 1$ and use the result of step one to express the variation of $df/d\kappa$ in terms of $\delta\kappa$. The latter result can then be used to analyze eventual singular behaviour of higher derivatives of the free energy.

Expanding the necessary condition (3.18) and using (3.21) we obtain for the variation of κ to lowest order

$$\frac{\delta\kappa}{\gamma} = -\frac{1}{2} \frac{\delta I}{(I_c)^3} - \frac{\lambda^c}{\gamma} \frac{M_c}{I_c} \left[\frac{\delta M}{M_c} - \frac{\delta I}{I_c} \right] = \left[\frac{-\pi^2}{256} + \frac{4}{3} \frac{\lambda^c}{\gamma} \right] \frac{\delta I}{I_c} - \frac{\lambda^c}{\gamma} \frac{\varepsilon}{2}, \quad (3.24)$$

where in the last step we made use of the relation (A.9) between the variations δI and δM and inserted the explicit results (A.5) for $I_c = I(1)$ and $M_c = M(1)$. Using the result (A.8) for $\delta I/I_c$ to lowest order we obtain

$$\delta\kappa = -\varepsilon \ln(\varepsilon) \sigma, \quad (3.25)$$

where we introduced the abbreviation

$$\sigma \equiv \frac{1}{8} \left[-\frac{\gamma\pi^2}{256} + \frac{4\lambda^c}{3} \right]. \quad (3.26)$$

Inverting equation (3.24) (again taking into account only the leading order) gives

$$\varepsilon = -\sigma^{-1} \delta\kappa \left[\ln(\sigma^{-1} \delta\kappa) \right]^{-1}. \quad (3.27)$$

This equation is the relation between the variation $\delta\kappa$ and ε which is implied by the necessary condition (3.18). In the final step we expand the derivative of the free energy (3.20) at $\mu = 1$ and use the result (3.27) to obtain the variation of the derivative in terms of $\delta\kappa$. Expanding (3.20) gives

$$\frac{df}{d\kappa} = -2\frac{M_c}{I_c} \left[1 + \frac{\delta M}{M_c} - \frac{\delta I}{I_c} \right] = -\frac{2}{3} - \frac{1}{3}\varepsilon \ln(\varepsilon) - \varepsilon. \quad (3.28)$$

Using (3.27) we obtain

$$\frac{df}{d\kappa} = -\frac{2}{3} + \frac{1}{3}\sigma^{-1}\delta\kappa + \sigma^{-1}\delta\kappa \left[\ln(\sigma^{-1}\delta\kappa) \right]^{-1}. \quad (3.29)$$

We remark, that the case $\mu < 1$ with expansion $\mu = 1 - \varepsilon$, $\varepsilon > 0$ changes only the sign of the argument of the logarithm. Differentiating the last result with respect to $\delta\kappa$ establishes the singular behaviour of the third derivative of the free energy with respect to κ . Thus we find a third order phase transition for $\mu = 1$. The critical line is a straight line given by (3.21).

It is important to notice, that at (see Equation (3.24))

$$\frac{\lambda^c}{\gamma} = \frac{3\pi^2}{1024}, \quad (3.30)$$

the leading term in the expression for $\delta\kappa$ vanishes. Equation (3.24) is reduced to the simpler relation

$$\frac{\delta\kappa}{\gamma} = -\varepsilon \frac{\lambda^c}{2\gamma}. \quad (3.31)$$

At this point the expansion of $df/d\kappa$ gives

$$\frac{df}{d\kappa} = -\frac{2}{3} - \frac{1}{3}\varepsilon \ln(\varepsilon) - \varepsilon = -\frac{2}{3} + \frac{2}{3\lambda^c}\delta\kappa \ln\left(-\frac{2}{\lambda^c}\delta\kappa\right) + \frac{2}{\lambda^2}\delta\kappa. \quad (3.32)$$

Again the case $\mu < 1$ differs only by the sign of the argument of the logarithm. Differentiation with respect to $\delta\kappa$ shows, that the phase transition has turned to second order at that point. Using (3.21) one can compute also the κ/γ coordinate of the second order point giving $\kappa/\gamma = \pi^2/1024$, $\lambda/\gamma = 3\pi^2/1024$. In fact the more global analysis in the next section will show, that the third order line terminates at the second order point $\kappa/\gamma = \pi^2/1024$, $\lambda/\gamma = 3\pi^2/1024$, and continues as a first order line.

3.4 Regime of the first order phase transition

As pointed out at the end of the last section at the point $\kappa/\gamma = \pi^2/1024$, $\lambda/\gamma = 3\pi^2/1024$, the third order transition along the $\mu = 1$ line (3.21) changes to second order. This unusual behaviour requires further investigation which we will carry out in this section. To begin, a graphical analysis of the phase diagram is most useful and in Figure 1 we plot a number

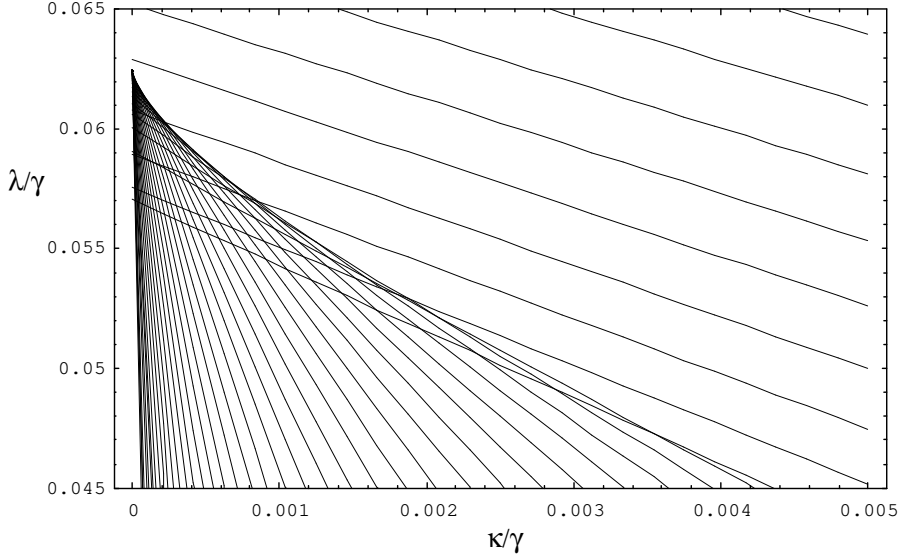


Figure 1: Plot of the lines (3.18) for μ ranging from 0.4 (upper right corner) to 75 (line at the extreme left). The region of overlapping lines corresponds to a region of first order phase transition.

of representatives of the family of lines (3.18) for a range of values of μ . It is clear that in most of the κ, λ -plane points are in a one-to-one correspondence with values of the parameter μ . This correspondence breaks down though in a small region near the λ/γ axis between $\lambda/\gamma = 0.05$ and $\lambda/\gamma = 0.0625$. Due to the behaviour of the slope and intercept in the linear equation (3.21) lines begin to overlap for increasing μ starting at $\mu \sim 1$ and continuing as $\mu \rightarrow \infty$. In this overlap region the phase diagram is folded at the vertex $\kappa/\gamma = \pi^2/1024$, $\lambda/\gamma = 3\pi^2/1024$, and each point falls on three different lines of constant μ . Consequently the system simultaneously admits three configurations with different free energies in this region of the phase space. This circumstance allows for a first order phase transition to develop along a line where the free energies of the different phases are equal.

The edges of the triangular first order region in Figure 1 is given by a caustic of lines from the one parameter family (3.18). The boundary is defined by the curve where the family of curves is stationary with respect to μ . This condition can be used with (3.18) to give a definition of the boundary caustic. The stationary condition can be solved with the parametric result

$$\frac{\kappa}{\gamma} = \frac{1}{4I^2(\mu)} \frac{I'(\mu)M(\mu) + M'(\mu)I(\mu)}{M'(\mu)I(\mu) - I'(\mu)M(\mu)}. \quad (3.33)$$

As can be seen, the curve given by (3.33) intersects the λ/γ axis at two points: 0.057024 ($\mu = 0.95324$) and $1/16$ ($\mu = \infty$) and reaches a singular maximum in the κ/γ direction for $\mu = 1$ at the point $\kappa/\gamma = \pi^2/1024$. The end of this region of first order transitions agrees with the position of the second order transition point which was determined by the analysis of critical behaviour in the previous section.

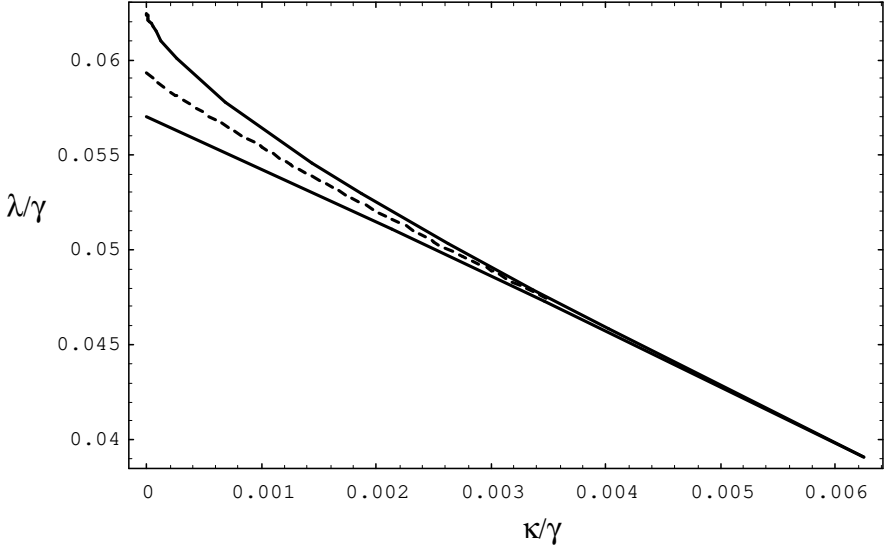


Figure 2: *Plot of the boundary of the multiple phase region. The boundary (solid curve) is given by a caustic of lines in the one-parameter family (3.18). The dotted curve shows the numerically determined first order line.*

Once one has determined the region where different phases can co-exist the next issue to address is that of the position of the line of first order phase transitions where different phases have the same free energy. This line can be determined for given κ/γ by the simultaneous solution for the parameters μ_1 and μ_2 of the pair of equations

$$\frac{I(\mu_2)M(\mu_2) - I(\mu_1)M(\mu_1)}{4 I(\mu_1)I(\mu_2)} = \frac{\kappa}{\gamma} [M(\mu_2)I(\mu_1) - I(\mu_2)M(\mu_1)], \quad (3.34)$$

and

$$\frac{1}{6} \left(\frac{\mu_1}{I^2(\mu_1)} - \frac{\mu_2}{I^2(\mu_2)} \right) - \frac{1}{12} \left(\frac{M(\mu_1)}{I^3(\mu_1)} - \frac{M(\mu_2)}{I^3(\mu_2)} \right) = \frac{\kappa}{\gamma} \frac{I(\mu_2)M(\mu_1) - M(\mu_2)I(\mu_1)}{I(\mu_1)I(\mu_2)}. \quad (3.35)$$

Unfortunately, these equations are analytically intractable. Again we turn to a graphical analysis to gain further insight. In Figure 3 we plot the free energy of the system as a function of λ/γ for different values of fixed κ/γ . From here it is easy to see a number of features of the region of first order transitions. Increasing μ traverses these curves in a clock-wise rotation so that free energy increases for small values of μ , intersecting the nearly horizontal large μ free energy. This intersection point is a graphical demonstration of the first order transition which occurs here as the model jumps from weak ($\mu < 1$) to strong coupling (μ large). Each phase continues to exist after the transition point and may be reached by an adiabatic process until ending in cusps which mark the boundaries of the first order region in the λ/γ axis. It is interesting to note that there is an energetically unfeasible intermediate “medium coupling” phase which connects the weak and strong phases. Hence, for fixed κ/γ there exist three distinct configurations of the system for given λ/γ in the region of first order transitions.

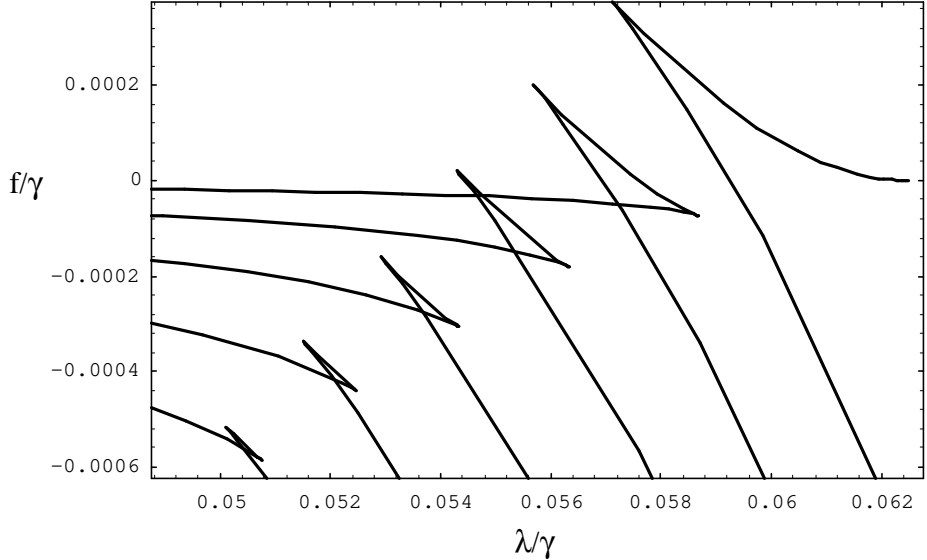


Figure 3: *Free energy in the region of first order phase transitions. Each curve is plotted for fixed κ/γ which from right to left is $\kappa/\gamma = 0, 0.0005, 0.001, 0.0015, 0.002, 0.0025$*

4 Discussion

We show that the whole phase diagram can be understood in terms of the energy densities of the fundamental charges the adjoint charges and the flux lines. Higher winding Polyakov loop operators will be used to characterize the phases of the model.

4.1 Energy densities

In this section we identify the expressions which should be interpreted as the energy densities of the fundamental charges the adjoint charges and the flux lines.

Using the definition (3.8) for the leading ($O(N^2)$) coefficient f of the density of the free energy we can formally denote the partition function $Z[T/e^2, \lambda_n, \kappa_n]$, defined in (2.15), (2.16) as (note that γ is related to T/e^2 via (2.18))

$$Z[T/e^2, \lambda_n, \kappa_n] \sim \exp(-N^2 L f(\gamma)) . \quad (4.1)$$

L denotes the space-like extension which is infinite. Thus (4.1) as it stands can only be understood formally, but could be made an exact identity by putting the system in a finite box. However, we show that derivatives of f have an interpretation as energy densities also in the infinite system.

Using (2.15), (2.16) we obtain

$$\frac{d \ln Z}{d T^{-1}} = -\langle H_{Flux} \rangle = -N^2 L \frac{df}{dT^{-1}} ,$$

where in the last step we made use of (4.1). Using the definition for γ (2.18) we obtain

$$\frac{df}{d\gamma} = \frac{1}{N^2} \frac{\langle H_{Flux} \rangle}{L} / e^2 \frac{N}{2} \equiv \rho_{Flux}. \quad (4.2)$$

ρ_{Flux} is the leading coefficient ($O(N^2)$) of the contribution of the electric flux to the energy density, measured in units of $e^2 N/2$. Note that $e^2 N/2$ is a proper unit for energy densities, since it is invariant in the limit $N \rightarrow \infty$ (compare (2.18)). The inclusion of the factor $1/2$ is natural, since the quadratic Casimir operator behaves (for $U(N)$) as $N/2$ at large N .

In the same way we can proceed to identify the contribution of the adjoint particles to the energy density²

$$-\frac{\lambda_J}{\gamma} \frac{df}{d\lambda_J} = \frac{1}{N^2} \frac{\langle H_{Ad} \rangle}{L} / e^2 \frac{N}{2} \equiv \rho_{Ad}. \quad (4.3)$$

Finally for the contribution of the fundamental charges and their conjugates we obtain

$$-\frac{\kappa_J}{\gamma} \frac{df}{d\kappa_J} = \frac{1}{N^2} \frac{\langle H_{F,\bar{F}} \rangle}{L} / e^2 \frac{N}{2} \equiv \rho_{F,\bar{F}}. \quad (4.4)$$

The differential equation (3.12) gives

$$\rho_{Flux} - \rho_{Ad} - \rho_{F,\bar{F}} = \frac{1}{\gamma} f = \frac{1}{N^2} \frac{F}{L} / e^2 \frac{N}{2}, \quad (4.5)$$

where F denotes the free energy of the system. Thus the density of the free energy is the difference of the contribution of the flux and the contribution of the charges.

When interpreting the phase diagram it is convenient to express the densities in terms of κ/γ , λ/γ , $I(\mu)$ and $M(\mu)$. Using (3.9), (3.19), (3.20) and (4.5) we obtain

$$\rho_{Flux} = \frac{1}{6I(\mu)^2} \left[\mu + \frac{M(\mu)}{I(\mu)} \right] - \frac{1}{96}, \quad (4.6)$$

$$\rho_{Ad} = \frac{\lambda}{\gamma} \left(\frac{M(\mu)}{I(\mu)} \right)^2, \quad (4.7)$$

$$\rho_{F,\bar{F}} = 2 \frac{\kappa}{\gamma} \frac{M(\mu)}{I(\mu)}. \quad (4.8)$$

The fact that ρ_{Flux} does not depend on κ/γ and λ/γ is most remarkable. It proves that the lines of constant μ are the lines of constant flux. In the last section we showed that the lines of constant μ are responsible for the structure of the phase diagram. This implies that the whole phase diagram can be understood by the abundance of flux.

We remark that the necessary condition (3.18) gives rise to another quantity which is constant on lines with fixed μ . It is the linear combination

$$\rho_{F,\bar{F}} + 2\rho_{Ad} = \frac{1}{2} \frac{M(\mu)}{I(\mu)^3}. \quad (4.9)$$

²Again we restrict ourselves to only one (real) pair $\lambda_J, \kappa_J \neq 0$, although some of the results of this section can be immediately taken over to the case of several nonvanishing couplings.

4.2 Higher windings of Polyakov loop operators

In addition to analyzing the phase diagram in terms of contributions of the electric flux and adjoint and fundamental charges to the free energy we also investigate higher windings of the Polyakov loop operators. As we will now demonstrate, their behaviour changes fundamentally at the line $\mu = 1$. It can be used to characterize the difference between the regions $\mu > 1$ and $\mu < 1$ and the physics in these different phases.

In the model with only the pair $\kappa_J, \lambda_J \neq 0$ we will be concerned with the quantities

$$P_k(\mu) \equiv \lim_{N \rightarrow \infty} \frac{1}{N} \langle \text{Tr} g^{k_J} \rangle = c_{k_J}. \quad (4.10)$$

Using (3.7), (3.13) and (3.14) we obtain

$$c_{k_J} e^{i\beta k_J} = \frac{M_k(\mu)}{I(\mu)}, \quad (4.11)$$

where we have defined

$$M_k(\mu) \equiv \frac{2}{\pi} \int_{-\pi}^{\pi} \cos k\theta \sqrt{\mu + \cos(\theta)} \text{H}(\mu + \cos(\theta)) d\theta. \quad (4.12)$$

Note that as in the cases of $I(\mu)$ and $M(\mu)$ (see Appendix A.2), we have performed a transformation of the integration variable which removes the dependence on J . The most important thing to note about this last equation is that these higher windings depend only on the parameter μ and hence give a unified picture of different regions of the phase space as does the electric flux density ρ_{Flux} .

In Appendix A.3 we show that the $M_k(\mu)$ and thus the higher windings of the Polyakov loop operators $P_k(\mu)$ undergo a drastic change of character at the point $\mu = 1$. We find, that for $\mu > 1$ they are exponentially suppressed with increasing k , while for $0 \leq \mu \leq 1$ there is only power law decay. Our results are (use (A.15), (A.13))

$$|P_k(\mu)| \leq (r(\mu))^k \frac{1}{2} \sqrt{2\mu + r(\mu) + r(\mu)^{-1}} \quad \text{for } \mu > 1, \quad (4.13)$$

with $r(\mu) \equiv (1 + \mu - \sqrt{\mu^2 - 1})/2 < 1$ for $\mu > 1$. For $\mu = 1$ we obtain

$$|P_k(\mu)| = \frac{1}{4k^2 - 1}, \quad (4.14)$$

and for $-1 \leq \mu < 1$ it is shown in Appendix 3.1 that exponential suppression is excluded.

In terms of a Fourier decomposition of the eigenvalue distribution $\rho_0(\theta)$, this result is a comment on the smoothness of the distribution. For $\mu > 1$, $\rho_0(\theta)$ has support on the entire circle and is infinitely differentiable, whereas for $\mu < 1$ the zeros of $\rho_0(\theta)$ with their infinite slope contribute higher frequencies to the Fourier series.

Physically one would like to be able to associate the change in behaviour of the higher winding Polyakov loops to a change in character of the gas of fundamental and adjoint charges. As seen above, and as will be expanded on in the next section, the phase diagram may be broadly divided into two regions. We have proven that $\mu = 1$ denotes a line of third order phase transitions up to a point where a first order line develops and there is a competition between phases with $\mu < 1$ and $\mu > 1$. Thus the behaviour of the $P_k(\mu)$ is different on both sides of the third order section of the critical line, as well as on the two sides of the first order section.

It is interesting to notice, that the large- k behaviour of the higher winding Polyakov loop operators $P_k(\mu)$ can also be interpreted as the long distance behaviour of a gauge invariant two-point function. In this picture $P_k(\mu)$ then corresponds to a Polyakov loop winding k -times around compactified time of the Euclidean model (compare (2.1)). Thus the $P_k(\mu)$ can be considered as the expectation value of a gauge invariant two-point function with time-like separation k/T , $k = 1, 2, 3, \dots$. For other models it was already proposed earlier [33], to use the changing decay properties of such operators as a confinement criterion.

It remains an interesting open question if the change in behaviour of the higher winding Polyakov loops persists in higher dimensions and for finite N . If it does, it would provide a powerful tool to study deconfinement transitions, in particular in lattice simulations, where the $P_k(\mu)$ are much simpler to analyze than other criteria, as e.g. the area law of the Wilson loop.

4.3 Physical interpretation of the phase diagram

Figure 4 gives a schematic plot of the phase diagram. In the following we explore the physical behaviour of the system in various regions of the phase diagram.

The line $\kappa = 0$ (purely adjoint model)

In the case of only adjoint charges (all $k_n = 0$) the action is invariant under transformations in the center of the gauge group, $g \rightarrow zg$ (compare (2.20)). When this symmetry is faithfully represented we expect

$$c_n(x) = \lim_{N \rightarrow \infty} \frac{1}{N} \langle \text{Tr } g^n(x) \rangle = 0 \quad \forall n \neq 0, \quad (4.15)$$

since

$$\text{Tr } g^n(x) \rightarrow z^n \text{ Tr } g^n(x).$$

From (3.3), (3.4) it is obvious that (4.15) which corresponds to constant eigenvalue density $\rho \equiv 1/2\pi$ is a solution. The stability analysis performed in [2] shows that this solution ("confined phase") is stable for $\lambda/\gamma \in [0, 1/16]$. Since the upper boundary of the multiple phase region is at $\lambda/\gamma = 1/16$ we confirm this result. The confined phase at $\kappa/\gamma = 0$

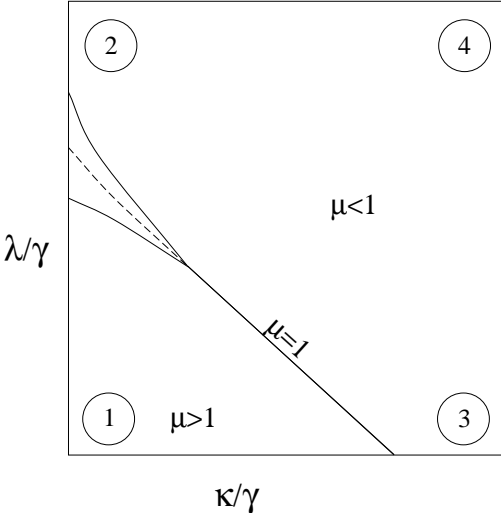


Figure 4: *Schematic picture of the phase diagram. The dotted curve marks the first order part of the critical line. The solid curves above and below it are the boundaries of the area with two possible phases. They join at a point which shows second order behaviour. For larger κ/γ we find a third order line ($\mu = 1$) marked by a solid line. The numbers label four extremal corners of the phase diagram, which we discuss below. We also indicate the range of the auxiliary parameter μ .*

corresponds to $\mu = \infty$ (compare Fig. 1). Inserting the results (A.10) for the large- μ expansion in (4.6), (4.7) and (3.19) respectively, we find energy densities $\rho_{Flux} = 0$, $\rho_{Ad} = 0$ and $f = 0$ in the confined phase of the purely adjoint model. Also the higher winding Polyakov loops $P_k(\mu)$ vanish as $\mu \rightarrow \infty$. All this supports the picture of adjoint charges being bound pair-wise in singlets under center transformations. The phenomenon of adjoint charges bound in such “hadrons” is called confinement.

For higher λ/γ the center symmetry is spontaneously broken. This corresponds to a solution, where the coefficients c_n are non-vanishing as well as the densities ρ_{Flux} , ρ_{Ad} and the energy density f . Typical values (taken at $\lambda/\gamma = 0.07$) are, $\rho_{Flux} = 0.017714$, $\rho_{Ad} = 0.020385$, $f/\gamma = -0.002671$. This “deconfining phase” has a nonvanishing overlap with the confining phase and gives rise to a phase transition which is of first order. The corresponding critical coupling can be computed numerically giving $\lambda/\gamma = 0.059250$. This result is in agreement with the value given in [2].

The line $\lambda = 0$ (purely fundamental model)

The center symmetry of the action is explicitly broken when there are fundamental charges (some $\kappa_n \neq 0$). In particular this is the case when we consider the model with only fundamental charges (and their conjugate). Thus we cannot expect to find a confining solution

with vanishing c_n which would correspond to vanishing densities ρ_{Flux} , $\rho_{F,\bar{F}}$.

For the purely fundamental model we have established the existence of a third order phase transition at $\kappa/\gamma = \pi^2/512$ (set $\mu = 1, \lambda = 0$ in (3.18)). The phase with κ/γ smaller than the critical value is characterized by low densities ρ_{Flux} , $\rho_{F,\bar{F}}$ and exponential suppression of the higher winding Polyakov loop operators $P_k(\mu)$, while for κ/γ greater than the critical value we find higher densities and power-like suppression of the $P_k(\mu)$.

Using the expansion (A.10) for large μ , one can compute the behaviour of the densities at small κ/γ . We obtain (expand (3.18) for large μ , to find the relation between κ/γ and μ)

$$\rho_{Flux} = 16 \left(\frac{\kappa}{\gamma} \right)^2 + O\left((\kappa/\gamma)^4\right) , \quad \rho_{F,\bar{F}} = 32 \left(\frac{\kappa}{\gamma} \right)^2 + O\left((\kappa/\gamma)^4\right) .$$

It is interesting to notice, that the two densities vanish with fixed ratio 2. This could be interpreted as a dilute gas of "hadrons" formed of pairs of fundamental charges and their conjugates bound together by flux.

The third order line

In Section 3.3 we established that at $\mu = 1$ there is a third order phase transition. For $\lambda/\gamma < 3\pi^2/1024$ the critical line is given by Equation (3.21). The third order behaviour terminates at $\kappa/\gamma = \pi^2/1024, \lambda/\gamma = 3\pi^2/1024$ becoming second order at that point, continuing as a line of first order transition. Using the values (A.5) we obtain for the energy densities of adjoint and fundamental charges

$$\rho_{F,\bar{F}} = \frac{2\kappa}{3\gamma} , \quad \rho_{Ad} = \frac{1\lambda}{9\gamma} .$$

The energy density of the flux is constant along the third order line and given by (evaluating (4.6) at $\mu = 1$)

$$\rho_{Flux} = 0.006718 .$$

The invariant linear combination (4.9) assumes the value

$$\rho_{F,\bar{F}} + 2\rho_{Ad} = 0.012851 ,$$

on the critical line.

The two phases above and below the third order line differ by the values of the energy densities, with higher values of density for large κ/γ and λ/γ . In particular the flux-density is higher for $\mu < 1$, and lower for $\mu > 1$. Thus we call the phase with $\mu > 1$ the "low density phase", while the other phase will be referred to as "high density phase". Since the energy density of the flux ρ_{Flux} vanishes entirely only for the purely adjoint model discussed in the last paragraph, we reserve the term "confined/deconfining phase" for this case.

The most dramatic change is seen in the behaviour of the higher winding Polyakov loop operators $P_k(\mu)$. We find exponential suppression with increasing k for $\mu > 1$ which corresponds

to the low density phase (small $\kappa/\gamma, \lambda/\gamma$). For $\mu < 1$ (high density phase) we showed that the $P_k(\mu)$ decay only power-like with k . On the critical line ($\mu = 1$) we find $|P_k(\mu)| = 1/(4k^2 - 1)$. Together with the behaviour of the flux density ρ_{Flux} , this allows to understand the whole phase diagram by the abundance of flux.

The first order line

The first order line comes about through the coexistence of two phases with equal free energy (compare Figure 3). The region where the phases coexist is shown in Figure 2. The two phases can be distinguished by the different contributions of flux and sources to the energy density (high density and low density phase). Typical values are (taken at $\kappa/\gamma = 0.002, \lambda/\gamma = 0.05203$)

$$\rho_{Flux} = 0.003328 , \quad \rho_{Ad} = 0.002811 , \quad \rho_{F,\bar{F}} = 0.000929 ,$$

for the low density phase which connects to the confined phase of the purely adjoint model ($\kappa/\gamma = 0, \lambda/\gamma \in [0, 1/16]$) and

$$\rho_{Flux} = 0.008999 , \quad \rho_{Ad} = 0.007856 , \quad \rho_{F,\bar{F}} = 0.001554 ,$$

for the high density phase which connects to the deconfining phase of the purely adjoint model ($\kappa/\gamma = 0, \lambda/\gamma > 0.057024$). Although unlike for the purely adjoint case, for $\kappa/\gamma > 0$ we have no immediate interpretation using symmetries, since for $\kappa/\gamma > 0$ the center symmetry is always broken explicitly. However, the physical behaviour in the first order region is still reminiscent of the purely adjoint case. The values of all three densities are considerably enhanced in the high density phase. Since the numbers we quoted are taken for a point on the critical line, they give rise to the same free energy (Note that the free energy is not the sum of the three contributions, but rather related to them by (4.5).).

It is important to notice, that also for the first order section of the critical line the higher winding Polyakov loops provide a criterion to distinguish the two phases. At the first order line a phase with $\mu > 1$ and a phase with $\mu < 1$ coexist. Thus also for the first order transition we find the characteristic exponential decay in the low density phase, but power-law behaviour in the high density phase.

The second order point

In the end of Section 3.3 it was established that the point $\kappa/\gamma = \pi^2/1024, \lambda/\gamma = 3\pi^2/1024$, which separates the third order part of the critical line from the first order part, is of second order. At this point the energy density for the adjoint and fundamental charges respectively are given by (insert $\mu = 1$ and the coordinates of the second order point in (4.7), (4.8))

$$\rho_{Ad} = \frac{\pi^2}{3072} , \quad \rho_{F,\bar{F}} = \frac{\pi^2}{1536} , \quad \frac{\rho_{F,\bar{F}}}{\rho_{Ad}} = 2 .$$

If one decreases κ/γ from its value at the second order point, the adjoint charges start to dominate, and the ratio $\rho_{F,\bar{F}}/\rho_{Ad}$ decreases - the first order region emerges. Conversely, with increasing κ/γ the fundamental charges start to dominate the system and $\rho_{F,\bar{F}}/\rho_{Ad}$ increases.

The existence of the phase transitions which we have discussed in this section is a bit surprising, considering the low dimensionality of the system. In fact, if we first consider the model with purely adjoint quarks as discussed in [2], there is a discrete symmetry under transformations in the center of the gauge group and the system is one-dimensional. Such a system cannot have a phase transition if N is finite. When N is infinite, the center symmetry becomes $U(1)$ and the group index behaves like another dimension, so the effective dimensionality of the model is two. In this case, the symmetry can be spontaneously broken (and there can be deconfinement) because the interaction potential has infinite range in eigenvalue space. This is also seen by considering the translation mode in eigenvalue space, which is the derivative by α of the eigenvalue density ρ . When the support of the density is a subset of the interval $[-\pi, \pi]$ the derivative of ρ is not a normalizable wavefunction (divergence in the norm coming from the edge of the distribution) for the zero mode and thus it is not effective in restoring the symmetry. Similarly, we expect that, when we turn on the density of fundamental representation quarks, the first or third order phase transition happens only at infinite N .

One can think of the infinite N limit here as something analogous to the infinite volume limit in the case of a ferro-magnetic system. In the latter, a phase transition in the mathematical sense only occurs when the volume is infinite. However, in the physically relevant case where the volume is large but finite, the phase transition is clearly seen. Similarly, in the present case of large N , the phase transition only occurs in the strict mathematical sense in the large N limit. It should nevertheless be visible when N is finite as long as finite size effects are not too large. One would expect that the tunneling which restores symmetry at finite N to be of order $\exp(-N^2 \cdot \text{const.})$ which could be very small even for rather small values of N . It would be very interesting to check this idea using lattice Monte Carlo simulations of these systems.

Extremal corners of the phase diagram

Finally we discuss extremal corners of the phase diagram, which are labeled 1,..,4 in Figure 4. Table 1 gives the values of κ/γ , λ/γ and the values of the contributions to the energy density. Obviously the four extremal cases can easily be understood by the magnitude of the energy densities ρ_{Flux} , ρ_{Ad} and $\rho_{F,\bar{F}}$. Point 1 is in the extremal corner of the low density phase. All three densities are rather small. Points 2 and 3 are both in the high density phase, in areas which are dominated by adjoint charges (Point 2) and fundamental charges (Point 3). It is nice to see, how the energy density of the sources is dominated by the contributions of the adjoint charges and fundamental charges respectively. Finally Point 4 is in a region where both the density of the adjoint charges as well as the fundamental charges is high and of the

same magnitude.

	1	2	3	4
κ/γ	0.00025	0.00025	0.25	0.25
λ/γ	0.000252	0.25	0.000251	0.25
ρ_{Flux}	1.033×10^{-6}	0.063260	0.072505	0.105058
ρ_{Ad}	4.064×10^{-9}	0.160997	0.000170	0.189518
$\rho_{F,\bar{F}}$	2.008×10^{-6}	0.000401	0.411543	0.435337

Table 1: *Values of $\kappa/\gamma, \lambda/\gamma$ and the contributions to the energy densities at four characteristic points in the phase diagram.*

It is interesting to notice, that when pushing the Points 2,3 and 4 to even higher values of κ/γ and λ/γ , one finds that the contribution of the charges to the energy density grows faster than the contribution of the flux. These extremal areas correspond to $\mu \sim -1 + \varepsilon$. Expanding the necessary condition (3.18) and the densities (4.6) - (4.8) for $\mu \sim -1 + \varepsilon$ (use (A.11)) we obtain

$$\rho_{Flux} = \left(\sqrt{\frac{\kappa}{\gamma} + \frac{\lambda}{\gamma}} \frac{\sqrt{2}}{6} - \frac{1}{96} \right) \left[1 + o\left(\sqrt{\kappa/\gamma + \lambda/\gamma}\right) \right],$$

$$\rho_{Ad} = \frac{\lambda}{\gamma} \left[1 + o\left(\sqrt{\kappa/\gamma + \lambda/\gamma}\right) \right], \quad \rho_{F,\bar{F}} = \frac{\kappa}{\gamma} 2 \left[1 + o\left(\sqrt{\kappa/\gamma + \lambda/\gamma}\right) \right],$$

in the limit $\kappa/\gamma, \lambda/\gamma \gg 1$. This shows that at very high energy densities, the contributions from the charges are dominating.

4.4 Summary

In this paper we analyzed the thermodynamic properties of a model of static sources on a line interacting through non-Abelian forces. It was shown that the partition function takes the form of the partition function of a gauged principal chiral model. Using the eigenvalue density as collective field variable the Hamiltonian for the eigenvalue density in the large N -limit was computed. We gave a static solution of the corresponding Hamilton equations. For the special case of only two types of charges, the static solution was parametrized using the parameter μ proportional to the Fermi energy. In particular the case of two types of charges transforming under the adjoint, and charges transforming under the fundamental representation of the gauge group was considered. Expanding the parametrized solutions at $\mu = 1$ we established the existence of a straight line in the phase diagram where the free energy exhibits a third order phase transition. We proved that the third order behaviour terminates at a second order point. The critical line then continues as a first order line, which was determined numerically.

The whole phase diagram was interpreted by analyzing the contributions of charges and flux to the energy density. We found that for $\mu > 1$ the system is characterized by low energy

densities, while for $\mu < 1$ the densities are high. The behaviour of higher winding Polyakov loop operators provides a powerful tool for a further characterization of the high and low density phases. In the low density phase we found exponential suppression with increasing winding number, while for the low density phase we proved a power-law behaviour.

It is tempting to analyze if the change of the behaviour of the Polyakov loops can be seen also in deconfining phase transitions in higher dimensions, and for finite N . If the picture persists, the Polyakov loop operators would provide a powerful criterion to analyze deconfinement phase transitions. In particular in lattice calculations this operator would be easier to analyze than other criteria as e.g. the area law of the Wilson loop operator.

Also the 2-dimensional model could be generalized in several directions. It would be interesting to analyze non-static solutions of the Hamilton equations and different boundary conditions which might be used to include a θ -term. Loop expansion of the fermion determinant of QCD_2 with large quark masses could be used to relate the fugacities of the non-Abelian gas analyzed in this article to the mass parameters of QCD_2 .

Acknowledgment

This work was supported in part by the Natural Sciences and Engineering Research Council of Canada. L. P. is supported in part by a University of British Columbia Graduate Fellowship.

Appendix

A.1 Cubic term in the Jevicki-Sakita Hamiltonian

In this section of the appendix we bring the second term on the left-hand-side of Equation (2.30) to a convenient form. The variation by $\rho(\theta)$ of this term is given by (up to a factor)

$$\mathcal{W}(\theta) = \left(\mathcal{P} \int d\theta' \rho(\theta') \cot \frac{\theta - \theta'}{2} \right)^2 - 2\mathcal{P} \int d\theta' \rho(\theta') d\theta'' \rho(\theta'') \cot \frac{\theta - \theta'}{2} \cot \frac{\theta' - \theta''}{2}.$$

In the integrals, we change variables to the complex variable

$$t = e^{i\theta} \quad , \quad t' = e^{i\theta'} \quad , \quad t'' = e^{i\theta''} \quad ,$$

so that the integrals are over an interval on the unit circle and

$$\mathcal{P} \int d\theta' \rho(\theta') \cot \frac{\theta - \theta'}{2} = \mathcal{P} \int \frac{dt'}{t'} \frac{t + t'}{t - t'} \rho(t') = i + 2\mathcal{P} \int dt' \frac{1}{t - t'} \rho(t') .$$

We obtain

$$\mathcal{W}(t) = 4 \left(\mathcal{P} \int dt' \frac{\rho(t')}{t - t'} \right)^2 - 8\mathcal{P} \int dt' dt'' \frac{\rho(t')}{t - t'} \frac{\rho(t'')}{t' - t''} + 1 - 4\mathcal{P} \int dt' dt'' \frac{\rho(t') \rho(t'')}{t'(t' - t'')} .$$

The last two terms are constants (which because of the normalization condition the the density $\rho(t)$ must satisfy, must be irrelevant), and the first term can be found by the following argument. We consider the function

$$G(z) = \int dt \frac{\rho(t)}{t - z} .$$

This function is analytic everywhere in the complex plane except on the arc of the unit circle where the eigenvalue density has support. Obviously

$$G(z) \rightarrow 0 \quad \text{as } |z| \rightarrow \infty .$$

Also, by letting z approach the support of $\rho(t)$ from outside and inside the unit circle, we obtain ($\varepsilon > 0$)

$$\lim_{\varepsilon \rightarrow 0} G(t(1 + \varepsilon)) \equiv G_+(t) = \mathcal{P} \int dt' \frac{\rho(t')}{t' - t} - i\pi \rho(t) , \quad (\text{A.1})$$

and

$$\lim_{\varepsilon \rightarrow 0} G(t(1 - \varepsilon)) \equiv G_-(t) = \mathcal{P} \int dt' \frac{\rho(t')}{t' - t} + i\pi \rho(t) , \quad (\text{A.2})$$

respectively. The function

$$K(z) = G^2(z) - 2 \int dt \frac{\rho(t)}{t - z} \mathcal{P} \int dt' \frac{\rho(t')}{t' - t} ,$$

is obviously analytic everywhere except eventually on the support of ρ . Using (A.1) and (A.2) one finds that it is continuous across the support of ρ since

$$\lim_{\varepsilon \rightarrow 0} K(t(1 + \varepsilon)) - \lim_{\varepsilon \rightarrow 0} K(t(1 - \varepsilon)) = 0.$$

Thus K is an entire function of z . Furthermore, since it vanishes at infinity, and is analytic everywhere

$$K(z) = 0.$$

Then, taking the real part of K on the support of ρ gives

$$\mathcal{W}(t) = 4\pi^2 \rho^2(t) + \text{const.} .$$

This is the functional derivative of the term

$$\frac{4\pi^2}{3} \int d\theta \rho^3(\theta) + \text{const.} , \quad (\text{A.3})$$

which is proportional to the second term in the Hamiltonian in the Schrödinger equation (2.31).

A.2 Analysis of the parametric integrals $I(\mu), M(\mu)$

Here we analyze the properties of the parameter integrals $I(\mu)$ and $M(\mu)$ originally defined in (3.15). A transformation of the integration variable brings the integrals to the form

$$\begin{aligned} I(\mu) &= \frac{4}{\pi} \int_0^\pi \sqrt{\mu + \cos(\theta)} H(\mu + \cos(\theta)) d\theta , \\ M(\mu) &= \frac{4}{\pi} \int_0^\pi \cos \theta \sqrt{\mu + \cos(\theta)} H(\mu + \cos(\theta)) d\theta , \end{aligned} \quad (\text{A.4})$$

which shows, that they are independent of J . $H(\cdot)$ denotes the step function. For $\mu = 1$ they can be evaluated explicitly, giving

$$I(1) = \frac{8\sqrt{2}}{\pi} , \quad M(1) = \frac{1}{3} \frac{8\sqrt{2}}{\pi} . \quad (\text{A.5})$$

For $\mu \geq 1$, the range of integration is $[0, \pi]$, while for $\mu < 1$, the step function reduces the range of integration to $[0, \arccos(-\mu)]$. $I(\mu)$ can be expressed in terms of complete $E(p)$ and incomplete $E(p; \phi)$ elliptic integrals

$$I(\mu) = \begin{cases} \frac{8\sqrt{\mu+1}}{\pi} E\left(\sqrt{\frac{2}{\mu+1}}\right) & \text{for } \mu \geq 1 \\ \frac{8\sqrt{\mu+1}}{\pi} E\left(\sqrt{\frac{2}{\mu+1}}; \arcsin\left(\sqrt{\frac{\mu+1}{2}}\right)\right) & \text{for } \mu \leq 1 \end{cases} . \quad (\text{A.6})$$

When expanding $I(\mu)$ and $M(\mu)$

$$\mu = 1 \pm \varepsilon, \varepsilon > 0 , \quad I(1 \pm \varepsilon) = I(1) + \delta_{\pm} I , \quad M(1 \pm \varepsilon) = M(1) + \delta_{\pm} M , \quad (\text{A.7})$$

one can use for $I(\mu)$ the well known formulas for the expansion of elliptic integrals (see e.g. [34]) to obtain

$$\frac{\delta_{\pm}I}{I(1)} = \mp \varepsilon \ln(\varepsilon) \frac{1}{8} \pm \varepsilon \frac{1}{8} [5 \ln(2) \pm 1] + o(\varepsilon). \quad (\text{A.8})$$

The variation $\delta_{\pm}M$ can be related to $\delta_{\pm}I$ by using

$$M(\mu) + \mu I(\mu) = \frac{4}{\pi} \int_0^\pi [\mu + \cos \theta]^{3/2} H(\mu + \cos(\theta)) d\theta.$$

Expanding the left hand side using (A.7) and the right hand side using Taylor expansion, one obtains

$$\frac{\delta_{\pm}M}{M(1)} = -3 \frac{\delta_{\pm}I}{I(1)} \pm \frac{3}{2} \varepsilon. \quad (\text{A.9})$$

We remark, that $I(\mu)$ and $M(\mu)$ have first derivatives that diverge logarithmically as μ approaches 1. This fact can be seen from (A.6), (A.9) and known formulas for the derivatives of elliptic integrals.

Finally we denote the large μ behaviour and the behaviour at $\mu \sim -1$. In both cases the results can be computed easily by expanding (A.4). We obtain

$$\begin{aligned} I(\mu) &= \sqrt{\mu} 4 \left[1 - \frac{1}{16} \frac{1}{\mu^2} + O(1/\mu^4) \right], \\ M(\mu) &= \frac{1}{\sqrt{\mu}} \left[1 + O(1/\mu^2) \right], \end{aligned} \quad (\text{A.10})$$

for $\mu \gg 1$, and

$$\begin{aligned} I(-1 + \varepsilon) &= \varepsilon \sqrt{2} + o(\varepsilon), \\ M(-1 + \varepsilon) &= \varepsilon \sqrt{2} + o(\varepsilon), \end{aligned} \quad (\text{A.11})$$

for $0 < \varepsilon \ll 1$.

A.3 Large k behaviour of $M_k(\mu)$

In this section of the appendix we analyze the large k behaviour of the higher moments $M_k(\mu)$ given by

$$M_k(\mu) = \frac{2}{\pi} \int_{-\pi}^{\pi} \cos k\theta \sqrt{\mu + \cos(\theta)} H(\mu + \cos(\theta)) d\theta. \quad (\text{A.12})$$

Again it is straightforward to evaluate the integrals at $\mu = 1$. We obtain

$$M_k(1) = \frac{8\sqrt{2}}{\pi} (-1)^{k+1} \frac{1}{4k^2 - 1}. \quad (\text{A.13})$$

For $\mu \neq 1$ no explicit solutions are available. For the case $\mu > 1$ we analyze the complex contour integral

$$I_C = \frac{2}{i\pi} \int_C z^{k-1} \sqrt{\mu + \frac{1}{2}(z + z^{-1})} dz. \quad (\text{A.14})$$

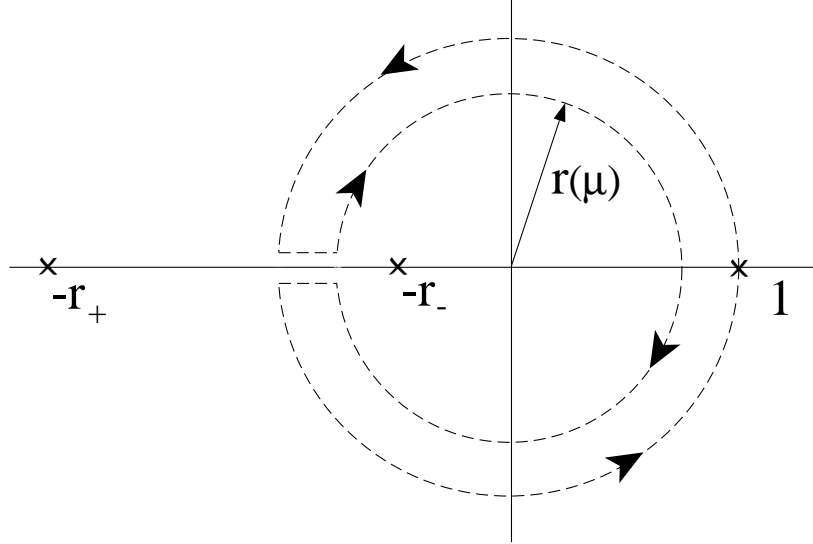


Figure 5: *Contour for the evaluation of the integral (A.14)*

For $\mu > 1$, the argument of the square root

$$f(z) \equiv \mu + \frac{1}{2}(z + z^{-1}),$$

can become real and negative, if and only if z is real and negative, i.e. $z = -r, r \geq 0$. In particular $f(-r)$ is zero for $r = r_{\pm} \equiv \mu \pm \sqrt{\mu^2 - 1}$, and $f(-r)$ is positive for $r_- < r < r_+$.

On the complex plane cut along the negative real axis $\sqrt{f(z)}$ exists uniquely and is holomorphic. If \mathcal{C} is a closed curve not crossing the cut, then $I_{\mathcal{C}}$ vanishes due to Cauchy's theorem. We choose a curve as shown in Figure 5. The outer circle is the unit circle, the inner one has radius

$$r(\mu) \equiv \frac{1}{2}(1 + \mu - \sqrt{\mu^2 - 1}).$$

The two pieces parallel to the real axis ($z = x + i\varepsilon$) cancel in the limit $\varepsilon \rightarrow 0$ (Note that $f(-r)$ has zeros at $r = r_{\pm}$. $r(\mu)$ was chosen to lie half way between -1 and $-r_-$, so that both integrals can be expanded in ε showing that they cancel each other.).

Thus we find that the integral along the inner circle equals the integral along the unit circle (both integrals evaluated in counterclockwise direction). $M_k(\mu)$ is given by the real part of $I_{\mathcal{C}}$ evaluated along the unit circle. Using the fact that the integral along the inner circle is bounded, we establish

$$|M_k(\mu)| \leq (r(\mu))^k \frac{4}{\sqrt{2}} \sqrt{2\mu + r(\mu) + r(\mu)^{-1}}. \quad (\text{A.15})$$

This proves that for $\mu > 1$ the moments $M_k(\mu)$ are exponentially suppressed with increasing k .

Finally we notice that for $-1 \leq \mu < 1$ exponential suppression is excluded by well known results of Fourier transformation. Using the fact that $M_k(\mu)$ is proportional to the Fourier coefficients of $\sqrt{\mu + \cos(\theta)}$ we find

$$\sqrt{\mu + \cos(\theta)} = \frac{1}{4}M_0(\mu) + \sum_{k=1}^{\infty} \frac{M_k(\mu)}{2} \cos(k\theta) .$$

The derivative with respect to θ then is given by

$$-\frac{1}{2} \frac{\sin(\theta)}{\sqrt{\mu + \cos(\theta)}} = -\sum_{k=1}^{\infty} k \frac{M_k(\mu)}{2} \sin(k\theta) .$$

If the $M_k(\mu)$ were exponentially suppressed, the series on the right hand side would converge to a finite constant for all θ . This contradicts the fact, that the left hand side diverges at $\theta = \arccos(-\mu)$ for $\mu < 1$. Thus for $-1 \leq \mu \leq 1$ (for $\mu = 1$ see the result (A.13)) we find only power-like suppression of $M_k(\mu)$ for large k .

References

- [1] Y. Nambu, B. Bambah and M. Gross, *Phys. Rev.* **D26** (1982), 2875.
- [2] G. W. Semenoff, O. Tirkkonen and K. Zarembo, *Phys. Rev. Lett.* **77** (1996), 2174; hep-th/905172.
- [3] G. W. Semenoff and K. Zarembo, Steklov Institute and UBC preprint, (1996); hep-th/9606117.
- [4] K. Zarembo, *Mod. Phys. Lett.* **A10** (1995), 677; hep-th/9405080;
K. Zarembo, *Teor. i Mat. Fiz.* **104** (1995), 25.
- [5] M. Billo, M. Caselle, A. D'Adda and S. Panzeri, preprint hep-th/9610144.
- [6] D. Gross and E. Witten, *Phys. Rev.* **D21** (1980), 446.
- [7] M. Douglas and V. Kazakov, *Phys. Lett.* **319B** (1993), 219; hep-th/9305047.
- [8] D. Gross and A. Matytsin, *Nucl. Phys.* **B437** (1995), 541; hep-th/9410054.
- [9] A. M. Polyakov, *Phys. Lett.* **72B** (1978), 477.
- [10] L. Susskind, *Phys. Rev.* **D20** (1979), 2610.
- [11] B. Svetitsky and L. Yaffe, *Nucl. Phys.* **B210** (1982), 423 ;
B. Svetitsky, *Phys. Rept.* **132** (1986), 1.
- [12] D. Kutasov, *Nucl. Phys.* **B414** (1994), 33; hep-th/9306013.
- [13] A. M. Polyakov, “Gauge Fields and Strings,” Harwood Academic Publishers, Chur, Switzerland, 1987.
- [14] V. Kazakov, *Soviet Physics JETP* **58** (1983), 1096.
- [15] I. Kostov, *Nucl. Phys.* **B265** (1986), 223.
- [16] D. Gross, *Nucl. Phys.* **B400** (1993), 161; hep-th/9212149;
D. Gross and W. Taylor, *Nucl. Phys.* **B400** (1993), 181; hep-th/9301068; *Nucl. Phys.* **B403** (1993), 395; hep-th/9303046.
- [17] A. M. Polyakov, Princeton preprint hep-th/9607049; Lectures at Banff Summer School on “Particles and Fields”, July 1994, unpublished.
- [18] S. Dalley and I. Klebanov, *Phys. Rev.* **D47**(1993), 2517; hep-th/9209049.
- [19] G. Bhanot, K. Demeterfi and I. Klebanov, *Phys. Rev.* **D48** (1994), 4980; hep-th/9307111;
D. Demeterfi, G. Bhanot and I. Klebanov, *Nucl. Phys.* **B418** (1994), 15; hep-th/9311015.

- [20] I. Kogan and A. Zhitnitsky, *Nucl. Phys.* **B465** (1996), 99; hep-ph/9509322.
- [21] R. Hagedorn, *Nuovo Cimento Suppl.* **3** (1965), 147;
 S. Fubini and G. Veneziano, *Nuovo Cimento* **64A** (1969), 1640;
 K. Huang and S. Weinberg, *Phys. Rev. Lett.* **25** (1970), 895.
- [22] J. Polchinski, *Phys. Rev. Lett.* **68** (1992), 1267; hep-th/9109007.
- [23] G. t'Hooft, *Nucl. Phys.* **B72** (1974), 461.
- [24] N. Weiss, *Phys. Rev.* **D35** (1987), 2495; A. Roberge and N. Weiss, *Nucl. Phys.* **B275** (1986), 734.
- [25] O. Borisenko, M. Faber and G. Zinoviev, preprint hep-lat/9604020.
- [26] D. Gross, R. Pisarski and L. Yaffe, *Rev. Mod. Phys.* **53** (1981), 43.
- [27] G. Grignani, G. W. Semenoff and P. Sodano, Perugia and UBC preprint (1995), hep-th/9504105;
 G. Grignani, G. W. Semenoff, P. Sodano and O. Tirkkonen, Perugia and UBC preprint (1995), hep-th/9511110; hep-th/9512048.
- [28] E. Langmann and G. Semenoff, *Phys. Lett.* **B296** (1992), 117; hep-th/9210011;
 E. Langmann and G. Semenoff, *Phys. Lett.* **B303** (1993), 303; hep-th/9212038.
- [29] E. Brezin, C. Itzykson, G. Parisi and J.-B. Zuber, *Comm. Math. Phys.* **59** (1979), 35.
- [30] A. Jevicki and B. Sakita, *Phys. Rev.* **D22** (1980) 467;
 S.R. Wadia, *Phys. Lett.* **93B** (1980) 403;
 S.R. Das and A. Jevicki, *Mod. Phys. Lett.* **A5** (1990), 1639.
- [31] S. Gubser and I. Klebanov, *Phys. Lett.* **B340** (1994), 35; hep-th/9407014;
 F. Sugino and O. Tsuchiya, *Mod. Phys. Lett.* **A9** (1994), 3149; hep-th/9403089;
 I. Klebanov and A. Hashimoto, *Nucl. Phys.* **B434** (1995), 264; hep-th/9409064.
- [32] S.R. Das, A. Dhar, A.M. Sengupta and S.R. Wadia, *Mod. Phys. Lett.* **A5** (1990) 891.
- [33] J. Bricmont and J. Fröhlich, *Phys. Lett.* **122B** (1983), 73;
 K. Fredenhagen and M. Marcu *Phys. Rev. Letters* **56** (1986), 223.
- [34] J. Spanier and K.B. Oldham, "An Atlas of Functions," Hemisphere Publishing Company, New York, 1987.